JOURNAL OF MATERIALS SCIENCE 17 (1982) 617–651

Review
The science of adhesion
Part 2 *Mechanics and mechanisms of failure*

A. J. KINLOCH
Ministry of Defence (P.E.), Propellants, Explosives and Rocket Motor Establishment, Waltham Abbey, Essex, UK

The previous paper, Part 1, reviewed surface and interfacial phenomena, including mechanisms of adhesion. The present paper, Part 2, reviews the mechanics and mechanisms of failure of adhesive joints and the effects of various operating environments on joint performance.

1. Introduction

In Part 1 [1] of this review the conditions necessary for establishing intimate interfacial contact between adhesive and substrate were considered and the reasons why materials should adhere together were discussed.

The present paper, Part 2, reviews the mechanics and mechanisms of failure of adhesive joints. Aspects of stress analysis and continuum fracture mechanics are discussed and these concepts are employed to explain the dependence of the measured joint strength upon such parameters as joint geometry, mechanical properties of the adhesive and substrates and test temperature and rate. It will be evident in these discussions that surface and interfacial aspects rarely enter into the argument, although these concepts are obviously essential in order to understand and be able to attain adequate adhesion. However, having established such adhesion, adhesive joints usually fail by cohesive fracture of the adhesive or substrates. An exception is the important problem of environmental attack on adhesive joints where the locus of failure is invariably at, or close to, the interface. Thus, in the review of environmental failure mechanisms the concepts introduced in Part 1 [1] will again play a decisive role.

2. Stresses in adhesive joints

Consideration is first given to the stress distribution in various common designs of adhesive joint. However, in order to predict the strength of adhesive joints, a knowledge of the stress distribution must be coupled with a knowledge of the relevant mechanical properties of the adhesive and substrate and a suitable failure criterion. Such criteria are not well established for adhesive joints but are discussed at the end of this Section.

2.1. Axially-loaded butt or poker-chip joints

This type of joint geometry is shown schematically in Fig. 1 and it might be supposed that the stress, σ_z, like the applied normal strain, e_z, is the same everywhere in the layer. However, this situation would only arise if, under the action of the normal stress, neither the substrates nor the adhesive tended to deform laterally or did so by the same amount, i.e., if the ratio of Poisson's ratio, ν, to Young's modulus, E, were the same for both materials. This condition is seldom, if ever, fulfilled since the ratio $\nu:E$ is usually higher for the adhesive so that the tendency for lateral deformation will be unequal in the two materials and this will give rise to stress concentrations.

Alwar and Nagaraja [2] and Adams *et al.* [3] have used an elastic finite-element method to analyse the stress distribution in butt joints loaded in tension and a typical stress distribution is shown in Fig. 2. The bonded area comprises two different regions.

First, in the central region, the tensile stresses are uniform and the shear stress, τ_{rz}, is zero. The

0022–2461/82/030617–35$06.70/0 © *1982 Chapman and Hall Ltd.*

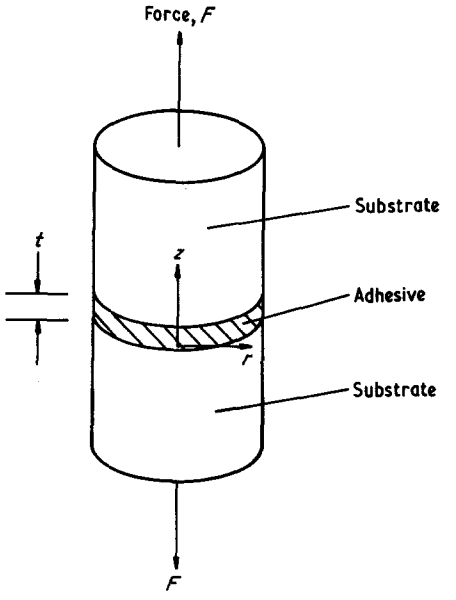

Figure 1 Sketch of axially-loaded butt or "poker-chip" joint.

radial, σ_r, and circumferential, σ_θ, stresses were found to be essentially the same as those predicted by the analysis of Kuenzi and Stevens [4]

$$\sigma_r = \sigma_\theta = \left[\nu_a - \frac{E_a \nu_s}{E_s}\right]\left[\frac{\sigma_z}{(1-\nu_a)}\right], \quad (1)$$

where the subscripts a and s refer to adhesive and substrate, respectively. For a rubbery material having a Poisson's ratio, ν_a, approaching 0.5 and bonded to a relatively rigid substrate (i.e., $E_s \gg E_a$) then, approximately,

$$\sigma_r = \sigma_\theta = \sigma_z. \quad (2)$$

Thus, in the central regions a hydrostatic tensile stress-state exists, a feature which has been appreciated for many years [5–7].

Second, around the periphery of the joint, there is a region where a shear stress, τ_{rz}, may be acting and where both shear and tensile stresses are dependent upon the ratio of the radius of the joint to the thickness of the adhesive layer, i.e., r/t. These stresses also vary across the adhesive thickness. On the mid-plane of the adhesive the tensile stresses decrease to low values at the free surface and the shear stress, $\tau_{rz}(z = 0)$, is always zero. At the adhesive–substrate interface there is a stress concentration at the edge of the substrate.

Harrison and Harrison [10] have examined the value attained by the interfacial shear stress, $\tau_{rz}(z = \pm t/2)$, for values of ν_a of 0.33 and 0.49. They have reported that a higher interfacial shear stress exists for the former case, but that in the latter case the stress is transmitted over a larger distance.

2.2. Single-lap joints

Of all the various geometries and methods of loading the single-lap joint loaded in tension has undoubtedly received the most attention from the stress analysts [8–30]. There are two main reasons for this interest. First, it is a convenient and thus frequently used test geometry for evaluating adhesives and, second, it is the basis for many joint designs employed in industry.

The single-lap joint loaded in tension is shown schematically in Fig. 3. The stresses in the adhesive layer are not, in practice, uniform and stress concentrations arise from the differential straining of the bonded substrates and from the eccentricity of the loading path.

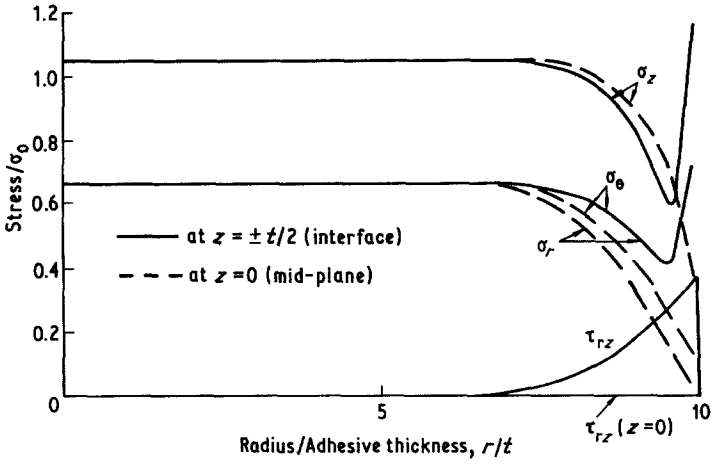

Figure 2 Stress distribution for butt joint loaded in tension. (σ_0 = average applied axial stress; $\nu_a = 0.4$; $E_a = 2.5$ GPa; $E_s = 69$ GPa; aspect ratio = 20) after Adams *et al.* [3].

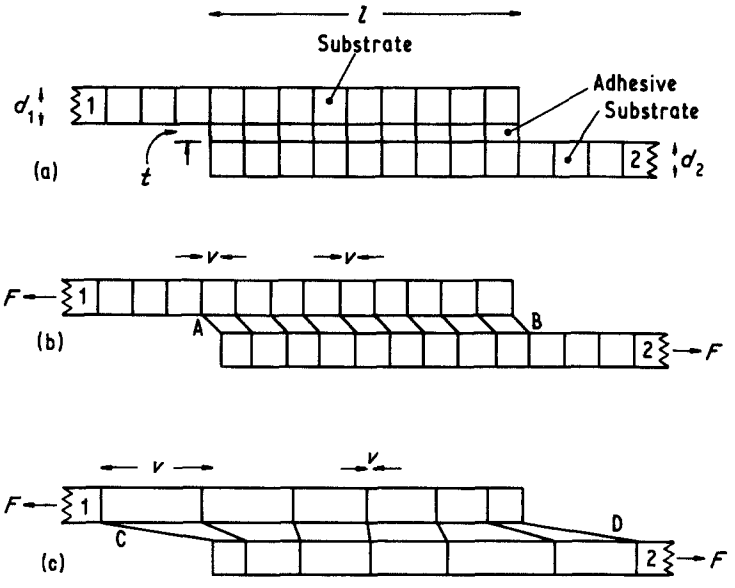

Figure 3 Schematic representation of single-lap joint. (v is the extension of adhesive). (a) Unloaded. (b) Loaded in tension, inextensible substrates. (c) Loaded in tension, elastic substrates.

The stresses arising from the differential straining of the bonded substrates were first studied by Volkersen [11] and may be understood [31] by reference to Fig. 3. In the case of the loaded joint with inextensible substrates, see Fig. 3b, the non-deformable substrates will move as solid blocks and the adhesive will suffer a uniform shear strain, γ_{yx}. However, each substrate bears the full load, F, just before the joint and transmits it gradually to the other through the adhesive. Thus, the stress in Substrate 1 will be highest at A and gradually diminish towards B where it will be zero and the converse will hold for Substrate 2. This variation in stress is not important if the substrates are inextensible but in practice, of course, they behave at least as elastic materials. Therefore, the picture of the deformation will be as in Fig. 3c and the largest deformations and shear strains, and hence stresses, in the adhesive will occur at the very ends of the overlap, at points C and D. (This cannot occur in practice since it implies a complementary shear stress on a free surface and no shear stress can exist on a free surface. Allowing for such end-effects appears to decrease the maximum shear-stress concentration, from that predicted for materials of Hookean elasticity, by a small amount [18].) For materials of Hookean elasticity the stress concentration factor, n, is given by:

$$n = \frac{\text{maximum shear stress}}{\text{applied shear stress}} = \frac{\tau_{yx}(\max)}{\tau_0} = (\Delta/W)^{1/2}\left(\frac{W-1+\cosh \Delta W}{\sinh \sqrt{\Delta W}}\right), \quad (3)$$

where

$$\Delta = \frac{G_a l^2}{E_{s2} d_2 t}, \quad (4)$$

$$W = (E_{s1}d_1 + E_{s2}d_2)/E_{s1}d_1, \quad (5)$$

if $E_{s1}d_1 > E_{s2}d_2$, and $\tau_{yx}(\max)$ is the maximum shear stress, τ_0 is the applied stress [$\tau_0 = F/$(bonded area) $= F/$(overlap-length $\times$ width)], G_a is the shear modulus of the adhesive, l is the overlap length, E_{s1} and E_{s2} are the Young's moduli of Substrate 1 and Substrate 2, respectively, d_1 and d_2 are the thicknesses of Substrate 1 and Substrate 2, respectively, and t is the thickness of the adhesive layer. For substrates for which $E_{s1}d_1$ and $E_{s2}d_2$ are equal then W reduces to a value of 2 and Equation 3 becomes [31]:

$$n = (\Delta/2)^{1/2} \coth (\Delta/2)^{1/2}. \quad (6)$$

Thus, the stress concentration factor becomes simply a function of a single dimensionless coefficient, Δ. It can, therefore, be readily appreciated that the theory of Volkersen predicts that decreasing the overlap-length or shear modulus of the adhesive, or increasing the stiffness of the substrate or the thickness of the adhesive layer, will decrease the shear stress concentration in the adhesive layer. However, whether these changes result in stronger joints will often depend upon other factors. For example, a decrease in G_a, possibly by plasticizing the adhesive, is usually accompanied by a decrease in shear strength of the adhesive, so little improvement may result from such a change in adhesive formulation.

The situation examined by Volkersen, whilst it indicates the importance of various parameters on the potential strength of a single-lap joint, is incomplete in that it takes no account of the tensile, or "tearing" stresses generated in the adhesive as a result of the eccentricity of the loading of the joint. This additional feature was first considered by Goland and Reissner [12] who recognized from laboratory experiments with lap joints that the bending of the substrates outside of the joint region has a pronounced effect upon the stress distribution in the joint itself. This effect they expressed in their bending moment factor, k, and associated rotation factor, k'. These parameters k and k' are not independent of one another but k is usually the dominant term; k, is dimensionless and is the ratio of the existing bending moment just before the bonded overlap to the value of this moment for inflexible substrates:

$$\frac{1}{k} = 1 + 2(2)^{1/2} \tanh \left\{ \left[\frac{3}{2}(1-\nu_s^2) \right]^{1/2} \frac{1}{2d} \left(\frac{\sigma_s}{E_s} \right)^{1/2} \right\}, \quad (7)$$

where ν_s and σ_s are the Poisson's ratio and applied stress for the substrate away from the overlap. Thus, k, depends upon the geometry of the joint, the elastic properties of the substrates and the stress on the substrates. The value of k is unity for undeformed substrates but, for increasing flexibility or load, k will diminish towards zero as a limit, although in practice it remains above about 0.35. Thus, as the substrates bend the value of k falls and the predicted stress concentrations in the joint decrease. Goland and Reissner [12] considered two cases:

(a) where the adhesive layer is extremely thin and of similar elastic stiffness to the substrates, so that its deformations are of little importance, for example, adhesive-bonded wooden joints; and

(b) where the layer is thin but its deformation makes a significant contribution to the stress distribution in the joint, as in bonded metal-to-metal joints.

Goland and Reissner [12] established the quantitative limits for these assumptions from strain-energy considerations.

For their first case, the stress distributions are shown in Fig. 4 and the variations of the maximum stresses with the bending moment factor, k, are shown in Fig. 5. As may be seen, the tensile (or tearing stress), σ_{yy}, is very high at the edge of the joint and all the stresses decrease as the bending moment factor, k, decreases, i.e., as the substrates bend.

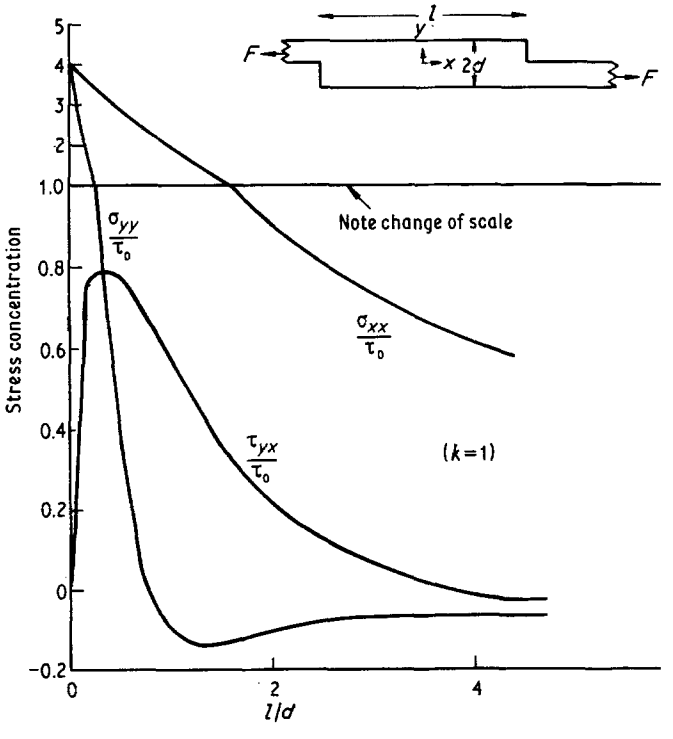

Figure 4 Stress distribution along the shear plane as a function of distance from the edge of the overlap (bending moment factor, k, equal to one), after Goland and Reissner [12].

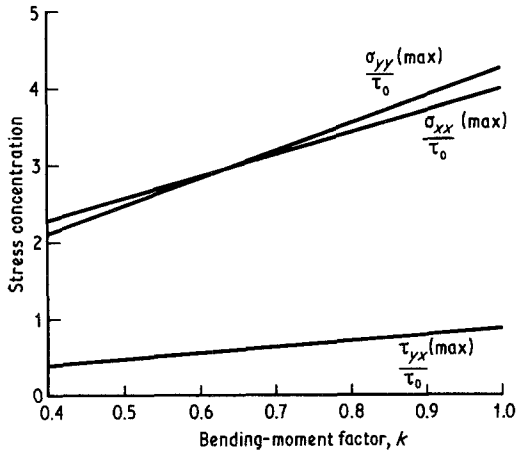

Figure 5 Reduction of the maximum stresses in the shear plane of a single-lap joint resulting from bending of the substrates (i.e., diminishing value of k), after Goland and Reissner [12].

For their second case,

$$\frac{\tau_{yx}(\max)}{\tau_0} = \frac{1+3k}{4}(2\Delta)^{1/2}\coth(2\Delta)^{1/2} + \tfrac{3}{4}(1-k), \quad (8)$$

and tensile stresses are also present in the adhesive layer. Thus, for relatively long overlaps and $k = 1$, Equations 3 and 8 reveal that the shear-stress concentration factor predicted by Goland and Reissner will be twice as large as that predicted from the analysis of Volkersen. This arises, of course, because the latter takes no account of the stress concentrations caused by eccentricity of the loading path.

Ishai *et al.* [32] have confirmed that for joints which exhibit essentially only elastic behaviour the analytical solutions of Goland and Reissner [12] are in good agreement with the experimental results for both the shear- and tensile-stress distributions in the adhesive layer.

So far only the stresses acting in two dimensions have been considered, but Adams and coworkers [16, 17] have approached the problem of examining the transverse stresses by experimental modelling and theoretical analytical and finite-element analysis solutions of the Volkersen theory considered in three dimensions. They demonstrated that Poisson's ratio strains generated in the substrates cause shear stresses in the adhesive layer and tensile stresses in the substrate acting perpendicular to the direction of the applied load. For metal-to-metal joints the transverse shear stress has a maximum value of about one-third of the minimum longitudinal shear stress, and this occurs at the corners of the overlap. This, therefore, enhances the shear-stress concentration which exists at this point due to the effects described above. Bonding substrates of dissimilar stiffnesses produces greater stress concentrations in the adhesive than when similar substrates are employed.

The above analyses all consider the substrates and adhesive to behave as elastic materials; however, most of the adhesives commonly employed exhibit elastic–plastic behaviour. Several groups of workers [8, 9, 19, 25–30, 33] have recently sought to include this behaviour in their calculations. The most extensive studies have been conducted by Hart-Smith [8, 25, 29] who has used closed-form analytical solutions, employing iterative solutions on a digital computer for the more complicated joint configurations. These studies show that inclusion of adhesive plasticity under shear loading in the analysis may decrease the stress concentrations substantially and thus increase the predicted joint strengths quite significantly, compared with a solely elastic analysis. However, the tensile stress, σ_{yy}, is often still moderately large. Hart-Smith advises that this feature, coupled with the low interlaminar tensile strength of composite laminates such as carbon-fibre reinforced-plastic (cfrp) and glass-fibre reinforced-plastic (grp), may cause premature failure by a delamination mechanism if composite materials are bonded employing a single-overlap joint design. He considers that such joints should not be used for primary structural bonding of composites, unless attached to a moment-resistant support to nullify the effects of the eccentricity in the loading path.

2.3. Double-lap joints

The double-lap joint is shown schematically in Fig. 6a and its symmetry results in much reduced normal stresses across the adhesive layer. However, even in symmetrical, double-lap joints the internal bending moments cause the normal stresses across the adhesive layer first considered by Volkersen [34] in a later analysis. Adams and Peppiatt [18] have recently employed an elastic finite-element analysis to joints containing an adhesive spew and have reported that the ratio of maximum principal stress in a single-lap joint (equivalent in dimensions to half the double lap) to that in the double-lap is 1.85. This was in good agreement with exper-

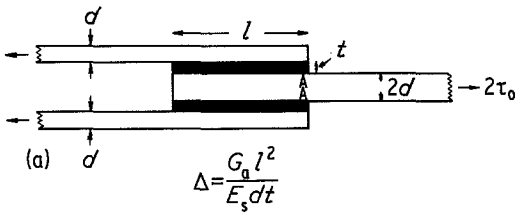

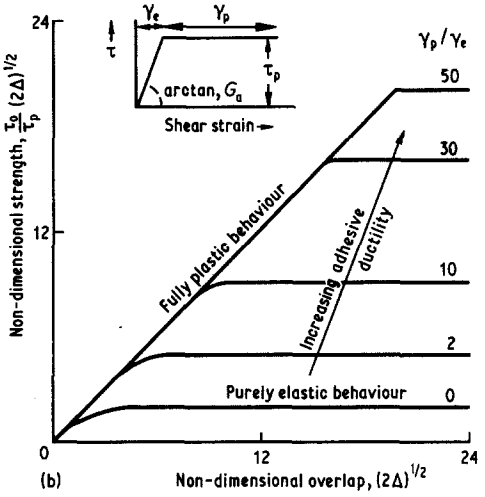

Figure 6 (a) Schematic representation of double-lap joint. (b) Shear-strength of balanced double-lap joints. Inset is diagram of shear stress–strain behaviour of adhesive; the subscripts e and p refer to elastic and plastic behaviour, respectively. After Hart-Smith [8, 25].

imental observations where the ratio of the half-failure load of a double-lap joint to the failure load of single-lap joint was 1.92.

Several authors [8, 9, 19, 25–30, 33] have considered the effect of adhesive plasticity and have shown that such behaviour reduces the calculated stress concentrations. Hart-Smith has conducted an extensive examination of this effect and Fig. 6b illustrates some typical results. The joint load is proportional to the overlap-length, l, for short overlaps but no further strength is to be gained by increasing the overlap beyond a certain point. The plateau strengths are given by

$$\frac{\tau_0(2\Delta)^{1/2}}{\tau_p 2} \rightarrow \left(1 + 2\frac{\gamma_p}{\gamma_e}\right)^{1/2}, \qquad (9)$$

where the parameters are defined in Fig. 6.

Hart-Smith also considered the tearing stresses, σ_{yy}, which are developed across the adhesive layer, and which are at a maximum at position A in Fig. 6a. He pointed out that these increase as the thickness of the outer substrate increases and beyond a certain thickness the tearing stresses exceed the peak shear stresses in magnitude. The presence of these high tearing stresses may cause a particular problem when bonding fibre-laminate materials whose interlaminar tensile strengths are comparatively low.

2.4. Modified-lap joints

Various modifications have been suggested to both the basic single- and double-lap shear joints in order to decrease their stress concentrations and so to raise the joint strength. Some typical examples from the work of Adams [9] are shown in Fig. 7.

The scarf joint [8, 9, 25, 31], and its variation the stepped scarf joint [25, 33, 35], are good examples of joints with low stress concentrations and also with zero weight penalty. Scarfing results in the differential strains, and hence the resulting stress concentrations, at the ends being considerably reduced. It also lowers the tearing stresses in the adhesive. These effects are particularly marked in the case of the scarf single-lap joints where this design greatly reduces the eccentricity of the loading path. Another variation on this theme is to taper the substrates on the outside of the joint [16, 31, 36, 37], as shown in Fig. 8a. This reduces the shear-stress concentrations but for the single-lap joint obviously has no effect on decreasing the eccentricity of the loading path. Furthermore, Thamm [36] has reported that tapering the substrates only yields a substantial increase in strength when the tapering is complete, i.e., the substrates are sharpened as far as possible to an edge. Partial sharpening, say to about half the original thickness, for example, is practically valueless from the strength view-point. In some instances the tapered substrates are reversed inwards [16], as shown in Fig. 8b. This results in a thicker adhesive layer at the ends of the overlap which may also assist in decreasing the stress concentrations (see Equations 3 to 6 and Fig. 6).

The double butt-strap lap joint has been studied in detail by Adams [3], Hart-Smith [25], Wright [38] and Sage [39] and the last three authors were particularly concerned with employing this joint geometry to bond cfrp materials. Sage [39] considered various modifications to the double butt-strap lap joint, such as tapering and radiusing the outside ends of the straps, and obtained joints which failed in the substrate completely, outside the joint, and were 100% efficient for strength.

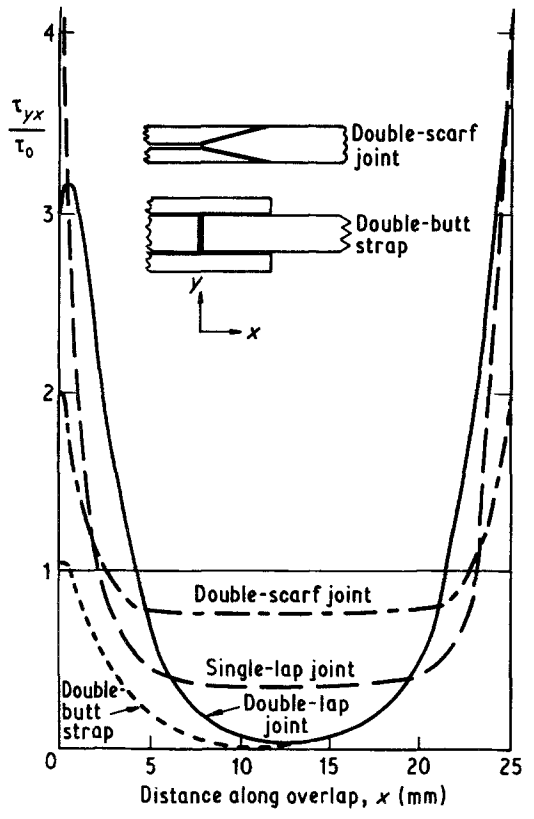

Figure 7 Shear stress concentrations for various lap-joint designs (elastic analysis for typical epoxy–aluminium-alloy joints), after Adams [9].

However, this design of joint does incur a weight-penalty.

2.5. Peel joints

The static stress distribution that results when a flexible member is peeled away from an adhesive layer supported on a rigid substrate has been considered by a number of authors [40–50] and reviewed by Bikerman [51] and more recently Wake [52]. These analyses have largely considered the adhesive and substrates as elastic materials and deduced the tensile and shear stresses in the adhesive layer. Kaelble [41] has shown that the tensile, or cleavage, stress, σ, at a distance, x, in the bond is given by

$$\sigma = \sigma_a(\cos \beta x + K_p \sin \beta x)e^{\beta x}, \quad (10)$$

where

$$\beta = \left(\frac{E_a H}{4E_s I t}\right)^{1/4}, \quad (11)$$

$$K_p = \frac{\beta m}{\beta m + \sin \alpha}, \quad (12)$$

σ_a is the boundary cleavage stress in the adhesive at $x = 0$ (i.e., the peel front), H is the width of the joint, I is the moment of inertia of flexible substrate cross-section, m is the moment arm of peel force and α is the peel angle.

Equation 10 assumes that the value of σ in the adhesive layer is constant through the adhesive thickness and across the width of the joint. It predicts that the distribution of cleavage stress is a highly-damped harmonic function involving alternating regions of tension and compression, a prediction that has been confirmed experimentally [42, 43]. Kaelble has also shown that the peel force, F_b, is given by

$$\frac{F_b}{H} = \frac{\sigma_a^2 t K_p^2}{2E_a(1 - \cos \alpha)}. \quad (13)$$

However, Gent and Hamed [53] have shown that the theory of small bending deformations used to derive Equation 10 is only applicable to peel mechanics when $\beta m \gg \sin \alpha$, i.e., when $K_p \approx 1$. The results from these analyses have not been widely employed in the interpretation of peel-test data and the energy-balance argument (see Sections 3.2.1 and 3.3.1.), which avoids the necessity for developing a detailed stress analysis has been far more widely applied.

More recently Crocombe and Adams [54, 55] have re-examined the problem of defining the stress distribution in the peel test. They have employed an elastic, but large-displacement, finite-element analysis approach and have reported that initial failure is caused by the principal tensile stresses in the adhesive driving a crack towards the interface between the adhesive and flexible substrate. Subsequent propagation was found to occur at a critical applied bending moment for a particular adhesive and substrate, independent of peel angle. Further, the load measured by the peel test was not proportional to the actual strength of the

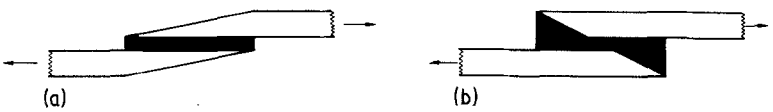

Figure 8 Examples of lap joints with tapered substrates.

adhesive, a small increase in the adhesive strength caused a much larger increase in the applied peel load.

2.6. Miscellaneous joint geometries

Adhesive bonding provides a convenient and light method of assembling structures consisting of thin-walled tubes and the stress distribution in such joints has been considered by several authors [34, 56–60]. Adams and Peppiatt [59] and Nagaraja and Alwar [60] have employed finite-element analysis techniques. The former authors examined the cases of both axial and torque loading and also considered the effects of *partial* tapering of the substrates to form a tubular scarf-lap joint. They concluded that, in agreement with Thamm [36], the reductions in stress concentration obtained did not justify its manufacture. Nagaraja and Alwar [60] assumed that the adhesive behaved in a non-linear fashion and found that the calculated stress concentrations were lower than those for the purely elastic adhesive assumption; maximum stress concentrations of about 1.3 were found for the dimensions and joint materials studied.

An annular butt joint or "napkin ring" specimen tested in shear minimizes the variation of shear stress in the adhesive and has been used by many workers to assess the shear strength and shear stress–strain behaviour of adhesives [6, 39, 61–66]. The shear-stress distribution calculated using simple elasticity theory is

$$\tau_{z\theta} = \frac{2Tr}{\pi(r_o^4 - r_i^4)}, \qquad (14)$$

where $\tau_{z\theta}$ is the shear stress at a radius r caused by an applied torque T, and where r_i and r_o are the inner and outer radii of the annulus, respectively. Adams *et al.* [5] used elastic finite element analysis to confirm that the shear stress does indeed increase linearly from zero at the centre to a maximum at the outside of a solid butt joint loaded in torsion. However, when they repeated the analysis allowing for an adhesive spew around the joint, as is usually found in practice, a greater shear-stress concentration occurred at the interface at the substrate corner, although the general level of shear stress was lower than that in a similar joint with no spew fillet. They concluded that if this type of joint was to be used to obtain the shear stress–strain curve for an adhesive, it should be tested without a spew fillet.

2.7. Internal stresses

Adhesives often operate with some additional stress in the joint arising from shrinkage of the adhesive relative to the substrates. The main reason for the shrinkage comes from equilibrium contact between the adhesive and substrates being established at temperatures above the subsequent operating temperature of the joint. Thus, since the adhesive and substrates usually have different coefficients of thermal expansion, thermal strains are introduced upon cooling. Other events such as polymerization reaction, cross-linking, loss of solvent, etc., may also be accompanied by volume contractions but are usually considered to be of secondary importance.

Experimental work [67–72], especially that using photoelastic techniques, has established the presence of residual stresses in joints but the results have often not been quantitative. For the simpler case of polymeric films coated onto metallic substrates, photoelastic techniques and a method based upon the bi-metallic strip principle have often been employed [73–78]. Using the latter method Danneberg [77] showed that for a wide range of epoxy-based coatings on an aluminium substrate thermal contraction was the major cause of internal stress and that the stresses generated were of the order of 0.08 MPa $^\circ$ C^{-1}.

The theoretical analysis of the internal stresses in an adhesive joint is beset with great difficulties even if it is assumed that the adhesive is perfectly elastic. Bikerman [79], Wake [80], Harrison and Harrison [10], Carlson and Sapetta [81] and Inoue and Kobatake [72] have made this assumption and attempted theoretical predictions. The maximum value of τ_{yx} occurs at, or near, an interface and near the ends of the joint, being zero in the centre. Harrison and Harrison have also concluded that τ_{yx}(max) is much higher for an adhesive possessing a Poisson's ratio of 0.33, as opposed to 0.49. Near the edges σ_{yy} is compressive while σ_{xx} falls below its value in the uniform stress region. However, these analyses all assume elastic behaviour and whilst the results from Inoue and Kabatake [72] appear intuitively to be of the expected magnitude, and were confirmed by photoelasticity techniques, the results from Carlson and Sapetta [81] appear to be unduly pessimistic. Indeed τ_{yx}(max) values calculated [82] from the Carlson and Sapetta analysis for an aluminium–epoxy–cfrp joint suggested that at low temperatures this joint would readily fail solely because of the high

internal stresses arising from thermal contraction. In practice, the joint possessed a relatively high strength. A more relastic, but still somewhat pessimistic, prediction of these experimental results is achieved if the analysis of Hart-Smith [25] is employed. This assumes elastic–plastic behaviour of the adhesive but makes no allowance for stress relaxation. Increased adhesive plasticity or adhesive layer thickness results in lower internal stresses.

Thus, to summarize, the magnitude and importance of internal stresses in adhesive joint is a frequently discussed topic and one which would certainly benefit from further studies.

2.8. Failure criteria

In order to predict the strength of adhesive joints a knowledge of the stress distribution in the joint must be coupled with a suitable failure criterion and the relevant mechanical properties of the adhesive.

Greenwood, Boag and McLaren [83] have suggested that the failure of lap joints occurs when the maximum shear stress in the adhesive layer attains the same value as the shear strength of the adhesive. Experimental results, using both a rigid, thermosetting adhesive and a flexible elastomeric adhesive were very encouraging but subsequent work [8, 9, 19, 25, 26, 33] has indicated that this criterion cannot be generally applied. These subsequent studies revealed that a criterion based upon maximum shear stress is insufficient since the strain capability of the adhesive, especially if it exhibits extensive plasticity when tested in shear, must be taken into account. Adhesives exhibiting elastic–plastic behaviour, rather than solely elastic behaviour, result in joints possessing lower stress concentrations, as discussed above, and do not fracture under shear loading as soon as the load corresponding to their shear strength. is attained. Thus, current practice is to use the maximum shear strain or maximum adhesive strain-energy in shear as the appropriate failure criterion. However, it should be noted that failure in lap joints may occur by modes other than shear failure of the adhesive. For example, the tearing stress, σ_{yy}, may exceed the tensile strength of the adhesive or the transverse strength of the fibre-composite substrate before any of the above conditions are met.

The difficulty in defining adequate failure criteria, even when equipped with a full knowledge of the stress distribution had led to the application of fracture mechanics to adhesive joint failure.

3. Fracture mechanics of adhesive joints

3.1. Introduction

Adhesive joints usually fail by the initiation and propagation of flaws and, since the basic tenet of continuum fracture mechanics theories is that the strength of most real solids is governed by the presence of flaws, the application of such theories to adhesive joint failure has received considerable attention.

Essentially, continuum fracture mechanics is the study of the strength of a structure which contains a flaw, usually considered as an elliptical crack. The theories were originally developed for cohesive fracture of materials [84, 85] but have been extended to adhesive joints, as discussed in recent reviews [86–88]. Two main, inter-relatable, conditions for fracture have been proposed.

First, the energy criterion, arising from the work of Griffith [89] and later Orowan [90], which supposes that fracture occurs when sufficient energy is released (from the stress field) by growth of the crack to supply the requirements of the fracture surfaces. The energy released comes from stored elastic energy or potential energy of the loading system and can, in principle, be calculated for any type of test-piece. However, even though, in principle, the energy release rate may be calculated, it may be difficult for some joint geometries and, hence, in order to measure this quantity suitable geometries have been developed which are discussed later. This approach therefore provides a measure of the energy required to extend a crack over unit area and this is termed the fracture energy or strain-energy release rate.

Second, Irwin [91] found that the stress field around a crack could be uniquely defined by a parameter named the stress-intensity factor, K, and stated that fracture occurs when the value of K exceeds some critical value, K_c. It should be noted that K is therefore a stress-field parameter independent of the material, whereas K_c, often referred to as the fracture toughness, is a measure of a material property.

3.2. Theoretical calculations

3.2.1. The energy-balance approach

The energy criterion for fracture is simply an extension of Griffith's hypothesis [89] which describes the quasi-static crack propagation as

the conversion of the work, W_d, done by the external force and the elastic energy, U, stored in the bulk of the sample into surface free energy, γ. For an increase in crack length, ∂a, it may be written

$$\frac{\partial(W_d - U)}{\partial a} \geqslant \gamma \frac{dA}{\partial a}, \tag{15}$$

where γ is the surface free energy per unit area, A is the interfacial area of the crack and a is the crack length. If the differentiation is carried out at a constant overall length, l, of the test-piece or, more precisely, if the external forces do no work since their points of application do not move, then, for a crack propagating in a lamina of width, H, the energy criterion for fracture becomes

$$-\frac{1}{H}\left(\frac{\partial U}{\partial a}\right)_l \geqslant 2\gamma. \tag{16}$$

Orowan [90] and Rivlin and Thomas [92] examined this criterion with respect to metals and cross-linked elastomers and commented that usually the energy required to cause crack growth is greater than the surface free energy. This is because in most real materials inelastic deformation mechanisms are usually operative. Such mechanisms include plastic, viscoelastic, etc., energy dissipative processes and are magnified by the relatively high strains experienced at, and close to, the crack tip. Thus, whilst elastic behaviour may be shown by the bulk of the material, inelastic deformations usually occur around the crack tip. The aforementioned authors assumed that such energy was dissipated in the immediate vicinity of the crack tip in a manner independent of the test arrangement and the manner in which forces were applied to it. Thus, 2γ may be replaced in Equation 16 by a parameter which encompasses all the energy losses incurred around the crack tip and is the energy required to increase the crack by unit length in a test-piece of unit width. This parameter is denoted by various symbols but in the present paper will be denoted by the symbol $\mathscr{G}_c$. (Note that in Part 1 [1] the symbol P was used.) Hence,

$$-\frac{1}{H}\left(\frac{\partial U}{\partial a}\right)_l \geqslant \mathscr{G}_c. \tag{17}$$

For structures exhibiting bulk linear-elastic behaviour, i.e., away from the crack-tip regions they obey Hooke's Law, Equation 17 becomes

$$\mathscr{G}_c = \frac{F_b^2}{2H}\left(\frac{\partial C}{\partial a}\right), \tag{18}$$

where F_b is the load required for crack propagation and C is the compliance of the structure and is given by displacement/load. Further, and most important, for an infinitesimally small amount of crack growth this equation is equally valid for a cracked body under fixed-extension or constant-load conditions.

However, the evaluation of Equation 17 is not necessarily restricted to those materials or structures which exhibit linear-elastic stress–strain behaviour. Rivlin and Thomas [92] have employed this approach to characterize the tearing of cross-linked elastomers which possessed bulk non-linear, but reversible elastic, properties. More recently, Gent *et al.* [93] have suggested that, even for elastomers which show significant internal energy dissipation outside of the immediate crack-tip regions, Equation 17 may still be used. However, the stored strain-energy available for crack propagation should not now be taken as the input energy but rather that deduced from the stress–strain relation upon retraction from the deformed state, i.e., the input energy minus the hysteresis (loss) energy. At a more fundamental level Rice [94] has developed the J-contour integral techniques for analysing materials which exhibit bulk non-linear-elastic behaviour and Andrews [95] has developed the generalized theory of fracture mechanics for non-linear and inelastic materials.

3.2.2. Stress-intensity factor approach

For a sharp crack in a uniformly-stressed infinite lamina and assuming Hookean behaviour and infinitesimal strains, Westergaard [96] has developed certain stress-functions which relate the local concentration of stresses at the crack-tip to the applied stress, σ_0. For regions close to the crack tip they take the form

$$\sigma_{ij} = \sigma_0\left(\frac{a}{2r}\right)^{1/2} f_{ij}(\theta), \tag{19}$$

where σ_{ij} are the components of the stress tensor at a point, r and θ are the polar co-ordinates of the point, taking the crack tip as origin, and $2a$ is the length of the crack. Irwin [91] modified this solution to give

$$\sigma_{ij} = \frac{K}{(2\pi r)^{1/2}} f_{ij}(\theta). \tag{20}$$

The parameter K is the "stress-intensity factor" and relates the magnitude of the stress-intensity load to the crack in terms of the applied loadings and geometry of the structure in which the crack is located. A crack may be stressed in three different modes, namely a tensile-opening, an inplane-shear and an antiplane-shear, and these are designated Modes I, II and III, respectively and are illustrated in Fig. 9. The tensile-opening or cleavage mode is technically the most important since it is the most commonly encountered and usually the one which most readily results in failure.

From Equation 20 it may be seen that as $r \to 0$ then the stress $\sigma_{ij} \to \infty$ and, hence, the stress alone does not make a reasonable local fracture criterion. Therefore, since the level of K uniquely defines the stress-field around the crack, Irwin postulated that the condition

$$K \geqslant K_c \tag{21}$$

represented a fracture condition; where K_c is a critical value for crack growth and, as such, is a material property and termed the fracture toughness.

The power of this approach is that for any problem K may always be expressed as, using Mode I as the example,

$$K_I = Q\sigma_0(\pi a)^{1/2}, \tag{22}$$

where Q is a factor dependent upon the exact geometry of the structure involved and K_I is the Mode I stress-intensity factor. Further, therefore,

$$K_{Ic} = Q\sigma_c(\pi a)^{1/2}, \tag{23}$$

where σ_c is the applied stress at the onset of crack propagation and K_{Ic} is the Mode I critical stress-intensity factor. Values of the geometry factor, Q, may be experimentally or theoretically ascertained and results for many geometries are listed in [97–100]. Hence, the fracture criterion embodied in Equation 21 may be employed by

(a) evaluating the value of K_I for the cracked structure under consideration from Equation 22, using realistic values of applied stress and flaw-size; and

(b) ascertaining the fracture toughness, K_{Ic}, of the material, or adhesive joint, employing standard laboratory test-specimens.

Finally, it should be noted that since the stresses at the crack-tip are singular then, clearly, the yield criterion is exceeded in some zone in the crack-tip region. If this zone is assumed to be small then it will not greatly disturb the elastic stress-field so that the extent of the plastic zone will be defined by the elastic stresses and Equation 22 and 23 will be essentially still valid. However, the assumptions of *bulk* elastic, small-strain behaviour cannot be so readily circumvented and so this approach is basically limited to rigid, glassy adhesives, such as phenolic and epoxy resin adhesives. Alternatively, the energy balance approach may be developed for both this type of adhesive and elastomeric (high-strain) adhesives, as mentioned above.

3.2.3. Relationship between the two approaches

The relationship between the fracture energy, $\mathscr{G}_c$, and the fracture toughness, K_c, have been derived [100, 101] for a crack in a homogeneous material and are given by

$$K_{Ic}^2 = E\mathscr{G}_c, \qquad \text{for plane-stress} \tag{24}$$

and

$$K_{Ic}^2 = \frac{E\mathscr{G}_c}{(1-\nu^2)}, \qquad \text{for plane-strain.} \tag{25}$$

If the other modes are considered then, in plane-strain [100]

$$E\mathscr{G}_c = (1-\nu^2)K_{Ic}^2 + (1-\nu^2)K_{IIc}^2 + (1+\nu^2)K_{IIIc}^2. \tag{26}$$

For a crack in an adhesive layer these relations embodied in Equations 24 and 25 have been

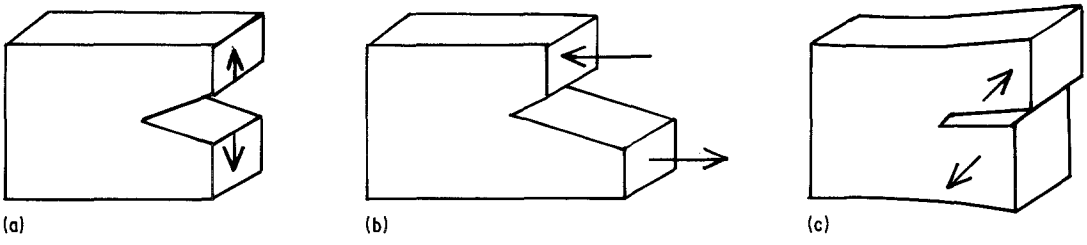

Figure 9 The three modes of crack growth: (a) tensile-opening; (b) inplane shear; (c) antiplane shear.

shown [102, 103] to be still generally valid and the appropriate value of the Young's modulus, E_a, of the adhesive may be employed to correlate K_c(joint) and $\mathscr{G}_c$(joint), albeit approximately in the case of very thin adhesive layers. However, Trantina [104] has shown that the value of $\mathscr{G}_c$ estimated from Equation 26 from adhesive joints where the ratio of Mode I and Mode II had been systematically altered (Section 3.3.2.) is not constant and therefore does not provide a useful failure criterion. This emphasises that interpretation of the stress-intensity factor for a crack at or near an interface is often more complex than for a homogeneous material. For example, even if the joint is subjected to only an applied uniform tensile stress the analysis may involve both Modes I and II values of K, although these values cannot be strictly associated with tensile and in plane-shear modes of failure, as they can for the homogeneous case [99, 104–107]. To overcome such problems several workers [107, 108] have defined an interfacial stress-intensity factor, K_i, as the characteristic parameter for a failure criterion and [107]

$$K_i = (K_I^2 + K_{II}^2)^{1/2}. \quad (27)$$

A further complexity is that significant differences may be observed in the stress-field from that predicted for the homogeneous material (Equation 20) outside a very limited distance ahead of the crack tip [103]. These difficulties with the exact interpretation of the stress-intensity approach have led many workers preferring to employ the energy-balance approach for crack growth in adhesive joints.

3.3. Experimental considerations

It is convenient to divide the experimental methods to deduce fracture mechanics parameters into those used when the adhesive joint is relatively rigid, as in structural adhesive joints, and those used when the adhesive joint possesses a fair degree of flexibility as, for example, in many rubber-to-metal joints.

3.3.1. Flexible joints

As discussed above, the energy-balance approach is the most applicable to flexible joints and the most common test method involves peeling the elastomeric adhesive away from a rigid support, as shown schematically in Fig. 10a. A detailed analysis has been published by Lindley [109] who assumed that when a force, F_b, was applied to the rubber tap of a peel test-piece at an angle α to the metal, the state of stress around the peel-front was independent of the amount of peeling which had taken place. He considered the energy balance before and after peeling of an amount, a, i.e., when a strip of rubber of unstrained length a is transferred from the unstrained state to the strained state. He argued that in this process (see also (i) to (iv) in Fig. 10a):

(i) The point of application of the force, F_b, will be moved a distance λa, where λ is the extension ratio of the rubber under the force, F_b. The work input is therefore, $F_b\lambda a$.

(ii) The rubber in the tab will have gained strain-energy $atHU_i$, where U_i is the strain-energy density in simple extension at extension ratio λ, t is the thickness of the tab and H is its width.

(iii) A horizontal force $F_b \cos\alpha$ is necessary to maintain equilibrium. The point of application of this force will move a distance a, requiring $F_b a \cos\alpha$.

(iv) An area of bond aH will have peeled required fracture energy per unit area, $\mathscr{G}_c aH$.

If no other external work is done the input energy (i) must be balanced by those of (ii), (iii) and (iv) giving

$$F_b\lambda a = atHU_i + F_b a \cos\alpha + \mathscr{G}_c aH. \quad (28)$$

Thus,

$$\mathscr{G}_c = \frac{F_b\lambda}{H} - \frac{F_b \cos\alpha}{H} - U_i t. \quad (29)$$

If the strain in the tab can be neglected then

$$\mathscr{G}_c = \frac{F_b}{H}(1 - \cos\alpha). \quad (30)$$

Hata *et al.* [110] have also derived Equation 29, in a somewhat different form, and Deraguin and Krotova [111] and Kaelble [40–42] (see Section 2.5) have obtained the simplified version embodied in Equation 30. In some instances the elastomeric adhesive is supported by a plastic backing-strip or the test geometry is changed so that a flexible substrate is peeled away from a flat, supported layer of adhesive. Under such circumstances it must be recognized that the stripping member may undergo plastic yielding if the bending stresses imposed by the peel force are sufficiently large. Plastic yielding provides an energy dissipation mechanism and thus a higher peel force is required than if yielding does not occur. This mechanism

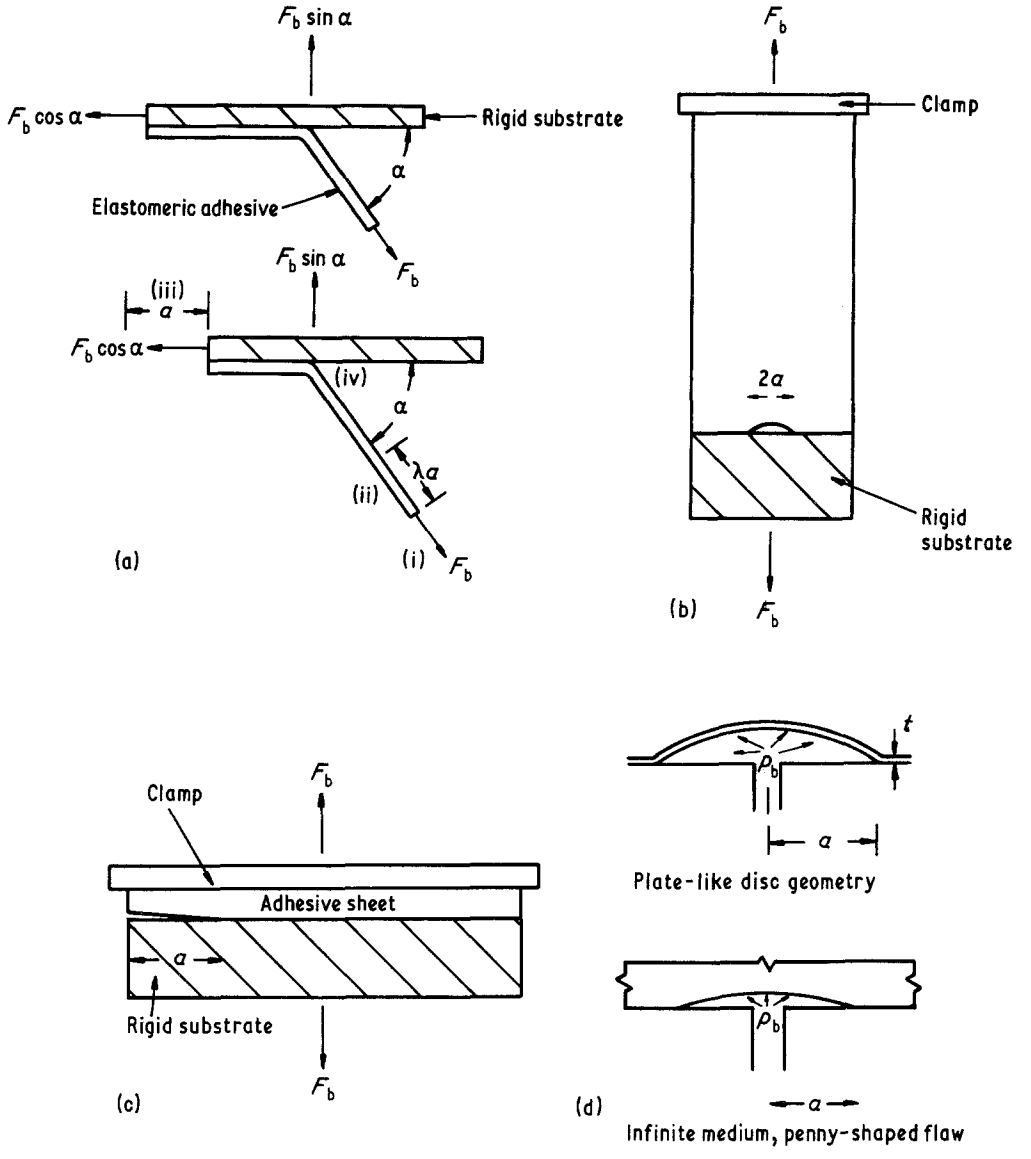

Figure 10 Adhesive joint geometries used for evaluating $\mathscr{G}_c$. (a) Peel test-piece before and after peeling by an amount, a. (b) Simple extension test-piece. (c) Pure-shear test-piece. (d) Blister test-pieces.

must be considered in an energy-balance analysis and the magnitude of this additional energy dissipation has been discussed by Gent and Hamed [53, 112].

As discussed above, a major feature of the fracture mechanics argument is that the fracture energy, $\mathscr{G}_c$, for a given joint, tested at a stated rate and temperature, is independent of the test geometry employed. Gent and Kinloch [113] and Andrews and Kinloch [114–116] employed the test geometries shown in Fig. 10a to c to verify that this was indeed true for a cross-linked styrene–butadiene rubber adhering to rigid substrates. The relations for determining $\mathscr{G}_c$ are [114]:

simple-extension test piece

$$\mathscr{G}_c = k'' a U_i; \tag{31}$$

pure-shear test piece

$$\mathscr{G}_c = t U_i, \tag{32}$$

where k'' is a numerical factor given by $\pi/\lambda_b^{1/2}$ where λ_b is the extension ratio of the rubber sheet for crack propagation. The simple-extension

geometry has also been used [117] to investigate the adhesion of epoxy resins, above their glass transition temperature, to metals.

Another configuration frequently employed for both flexible and rigid joints is the "pressurized blister-test", shown in Fig. 10d. The specimen configuration was originally suggested by Danneberg [118], amplified in certain analytical respects by Malyshev and Salganik [119] and subsequently considerably developed by Williams and co-workers [120–124] and Anderson *et al.* [125]. In its simplest form it consists of a disc or plate which has been cast, and hence adhered, against a rigid substrate, except for a central portion of radius, a. When the unbonded region is pressurized, as by the injection of compressed air or fluid, the plate lifts off the substrate and forms a blister whose radius stayed fixed until a critical pressure, p_b, is attained. At this value the radius of the blister increases in size, i.e., a crack-growth occurs. In principle, any thickness or diameter of disc and any de-bond radius smaller than the disc may be used. However, analytical closed-form engineering solutions for the displacement are currently available only for the near-limit cases of a disc using plate theory and the infinite isotropic medium adhering to a rigid substrate with a small penny-shaped de-bond between the two materials. Assuming linear-elastic behaviour:

for plate-like disc geometry

$$p_b = \left[\frac{32}{3(1-\nu_a^2)}\left(\frac{t}{a}\right)^3\right]^{1/2}\left(\frac{E_a \mathscr{G}_c}{a}\right)^{1/2}; \quad (33)$$

for any infinite medium penny-shaped flaw ($\nu_a = 0.5$)

$$p_b = \left(\frac{2\pi}{3}\right)^{1/2}\left(\frac{E_a \mathscr{G}_c}{a}\right)^{1/2}. \quad (34)$$

Andrews and Stevenson [126] have recently expressed these equations as

$$\mathscr{G}_c = \left(\frac{1}{f(t/a)}\right)\left(\frac{p_b^2 a}{E_a}\right) \quad (35)$$

and evaluated the function of $f(t/a)$ over a wide range of t/a values for cracks propagating both along the interface and cohesively through the adhering layer. Williams and co-workers [121, 122, 127] have also considered the case for an elastic adhesive interlayer between the plate and rigid substrate. Further, a first-order correction for the effect of viscoelasticity has been suggested [127, 128] by replacing the constant elastic modulus, E_a, by the stress–relaxation modulus $E_a(t_f)$ evaluated at the appropriate time-scale, t_f. The pressurized blister-test has found many diverse applications such as for assessing the adhesion of various dental cements and teeth [129], explosively-welded plates [130], paints [131], barnacle cement [13] and solid-propellant rocket motors [127, 132]. However, Anderson *et al.* [124] have commented that the value of the adhesive fracture energy, $\mathscr{G}_c$, may not be completely independent of the geometry of the blister-test method since the loading mode changes for largely Mode I to a combination of Modes I and II if the specimen thickness to initial debond radius ratio is decreased. However, a constant Mode I value of $\mathscr{G}_c$ was obtained when t/a was greater than about one.

Various other geometries have been developed to determine $\mathscr{G}_c$ for elastomeric adhesives including cone-test specimen [124], a torsion test (resulting in Mode III failure) [124] and the adherence of spheres of the elastomer [133–136].

Some typical values of adhesive fracture energy, $\mathscr{G}_c$, of a polyurethane elastomer–polymethylmethacrylate interface, tested at room temperature and at a moderate rate of test, are shown in Table I. These values will, of course, be highly dependent upon test temperature and rate, as discussed in Part 1 [1].

3.3.2. Rigid joints

The various designs which have been employed to determine the adhesive fracture energy, or fracture toughness, of relatively rigid joints have been recently reviewed by Kinloch and Shaw [87]. The pioneering work in the application of continuum fracture mechanics of crack growth in such joints was conducted by Mostovoy, Ripling and Patrick [137, 138]. They employed a double-cantilever-beam and a shear specimen, as shown in Fig. 11a and b, to determine the values of $\mathscr{G}_{Ic}$ and $\mathscr{G}_{IIc}$ of epoxy–aluminium-alloy joints. However, the most popular design for ascertaining Mode I values has

TABLE I Values of adhesive fracture energy, $\mathscr{G}_c$, of a polyurethane–polymethylmethacrylate interface [124]

Test geometry	Mode of failure	$\mathscr{G}_c$ (kJ m^{-2})
90° peel	I	0.032
Blister – $t/a > 1$	I	0.030
Blister – $t/a \ll 1$	II	0.072
Torsion	III	0.10

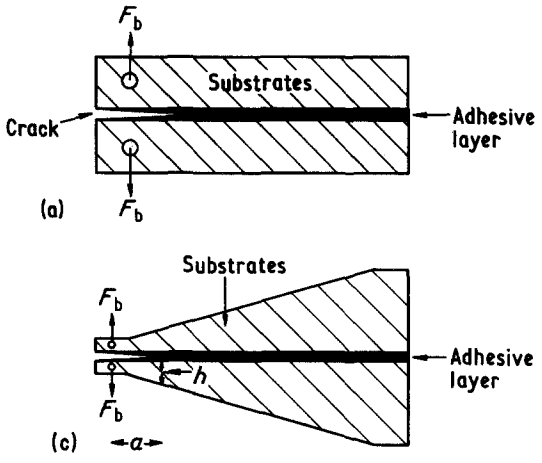

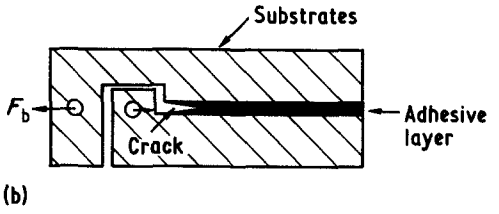

Figure 11 Adhesive joint geometries used to determine $\mathscr{G}_c$-values of structural adhesives. (a) Parallel-double-cantilever-beam (Mode I); (b) shear specimen (Mode II); (c) tapered-double-cantilever-beam specimen (Mode I).

been the tapered-double-cantilever-beam specimen, shown in Fig. 11c.

The tapered-double-cantilever-beam joint design was developed by Mostovoy and Ripling [139] and if the arms of the specimen behave in a linear elastic manner then

$$\mathscr{G}_{Ic} = \frac{F_b^2}{2H}\left(\frac{\partial C}{\partial a}\right). \tag{36}$$

The value of $\partial C/\partial a$ may be found experimentally but Mostovoy, Crosley and Ripling [140] showed that

$$\frac{\partial C}{\partial a} = \frac{8M}{E_s H}, \tag{37}$$

where M is the geometry factor and is given by

$$M = \frac{3a^2}{h^3} + \frac{1}{h}, \tag{38}$$

where h is the height of the beam at the respective crack length, a. The aim of tapering the substrates is to maintain the geometry factor, M, constant along most of the length of the specimen so that the value of $\partial C/\partial a$ is constant. Thus, at a given applied load the value of $\mathscr{G}_{Ic}$ will be independent of crack length. Herein lies the main advantage of this geometry, namely, the value of $\mathscr{G}_{Ic}$ may be readily calculated without a knowledge of the crack length and this is particularly useful since the crack tip is often difficult to define accurately in adhesive specimens, especially during environmental testing.

A variant on the above specimen design is one where the width of a parallel-double-cantilever-beam is increased down the length so that $\partial C/\partial a$ is again constant [141, 142]. This design has been most successfully employed to ascertain $\mathscr{G}_{Ic}$ values for interlaminar fracture of glass- and carbon-fibre composites [143]. The double-torsion joint [144, 145] is another geometry where $\partial C/\partial a$ is constant. The blister specimen (Fig. 9d) has been used for structural adhesive joints [126, 146–148] and the value of the adhesive fracture energy obtained is truly a plane-strain value. This may be a useful aspect since, if a significant amount of plane-stress failure occurs, then a higher value of $\mathscr{G}_c$ may be deduced which may lead to an optimistic failure prediction. However, fracture mechanics tests usually require crack growth to proceed from a sharp crack and it is extremely difficult to insert sharp initial cracks, or debonds, into the blister specimen; blunt cracks may lead to artificially high values of $\mathscr{G}_c$. Also, unless the adhesive is transparent, it is difficult to monitor the rate of crack growth in the blister specimen.

Bascom and co-workers [149] have commented that for isotropic materials Mode I is the lowest energy fracture mode and thus a crack will always propagate along a path normal to the direction of maximum principal stress. Hence, a crack in an isotropic plate will propagate in Mode I facture regardless of the orientation of the initial flaw with respect to the applied stress. However, this is not necessarily the case in joint fracture since crack propagation is constrained to the adhesive layer regardless of the orientation of the adhesive layer, except of course when the substrate has a lower toughness than the adhesive. Thus, for structural design purposes attention must be given to joint fracture under additional loading modes. Several designs have been developed for measuring Mode II values [137, 138, 150–152] and also for studying joint fracture under combinations of Modes I and II [152–154] and even Mode III failure [142].

Apart from the mode of failure the measured adhesive fracture energy has been shown to be dependent upon adhesive composition [139, 155, 156], including the incorporation of rubber-toughening particles [149, 157–164], the test temperature and rate [135, 146, 155, 156, 161, 162, 165–167] and the presence of hostile environments [87, 144, 147, 168–194]. The principal substrate materials employed have been aluminium-alloys, in support of the aerospace industries, but steel [161], glass [168] and wood [175, 176] have been used and the influence of substrate surface pretreatment has also been investigated [153, 154, 162, 172, 174, 176–178]. Thus, it is difficult to state values of $\mathcal{G}_c$ for adhesive joints without defining the exact details of the adhesive, substrate and test parameters; however, an attempt is made in Table II to impart an idea of the range of the values that may be observed.

As may be seen from Table II, structural adhesives possess relatively low values of fracture energy, $\mathcal{G}_{Ic}$, even when they are formulated with a rubber toughening agent. This is, of course, a consequence of their high cross-link-density and high inter-chain attractive forces which impart the desirable properties of relatively high modulus, good temperature resistance and low creep behaviour. However, the values of $\mathcal{G}_{Ic}$ are still at least one hundred times the energy required to break solely covalent bonds (less than $1\,J\,m^{-2}$) which demonstrates that other energy absorbing processes, such as viscoelastic and plastic deformations, must take place at the crack tip. These mechanisms have been clearly identified by examining the fracture surfaces of failed adhesives using scanning electron microscopy [179–181].

4. Measuring the strength of adhesive joints

4.1. Standard test methods

The commonly used standard test methods are those issued by the British Standards Institution (BS series) or the American Society for Testing of Materials (ASTM series). They are listed in Table III.

4.2. Effect of joint geometry

4.2.1. Axially-loaded butt joints

Bryant and Dukes [182] have demonstrated that the fracture stress, σ_b, of axially-loaded butt joints is independent of the diameter of the substrate, over a wide range of diameters and for relatively thin adhesive layers, for joints employing either a rigid, epoxy or rubbery, silicone adhesive. However, in accord with other workers [183–189] they reported [182, 190] that the fracture stress increased as the thickness of the adhesive layer decreased. Until recently, the favoured explanations for this effect were based either upon the presence of higher internal stresses [80, 191] or upon the statistical probability of larger flaws [183, 189, 190] in the joints employing relatively thick adhesive layers. However, recent elegant work by Gent [86, 192] and Hilton and Gupta [193] has demonstrated that a fracture-mechanics approach to this problem provides a simple, and even quantitative, mechanism for this effect.

Gent [192] has examined the strength of butt joints consisting of an elastomeric adhesive bonding relatively rigid substrates and tested over a wide range of temperatures and rates. The results were found to yield a single master relation in terms of the reduced deformation rate, $\dot{e}a_T$, by means of the Williams, Landel and Ferry rate–temperature equivalence for viscous materials

TABLE II Typical values of adhesive fracture energy, $\mathcal{G}_c$, for some structural adhesive joints. (All tests conducted at room temperature and at moderate test rates)

Joint*	$\mathcal{G}_{Ic}$ ($kJ\,m^{-2}$)	$\mathcal{G}_{IIc}$ ($kJ\,m^{-2}$)	Reference
DGEBA-TEPA–Aluminium alloy	0.07	1.45	[138, 156]
DGEBA-TEPA–Aluminium alloy in aqueous environment	0.015	–	[168]
DGEBA-3° amine–Aluminium-alloy	0.10	–	[156]
DGEBA-HHPA–Aluminium-alloy	0.10	–	[165]
DGEBA-PIP-CTBN–Aluminium-alloy	3.40	3.55	[154]
Phenol-resorcinol–Maple	0.1	–	[176]

*Resin: DGEBA, diglycidyl ether of bisphenol A

Curing agents: TEPA, tetraethylene pentamine; 3° amine, tertiary amine salt; HHPA, hexahydrophthalic anhydride; PIP, piperidine.

Rubber toughening agent: CTBN, carboxyl-terminated-butadiene-acrylonitrile rubber.

Note (for comparison): $\mathcal{G}_{Ic}$(polystyrene) = $0.4\,kJ\,m^{-2}$; $\mathcal{G}_{Ic}$(high-impact polystyrene) = $16\,kJ\,m^{-2}$; $\mathcal{G}_{Ic}$(7075 aluminium alloy) = $20\,kJ\,m^{-2}$.

TABLE III Standard test methods for adhesive joints

Test	Standard	Comments
Axially-loaded butt joints	BS 5350: Part C3: 1979	
	ASTM D897-78	
	ASTM D2094-69 and D 2095-72	Specifically for bar- and rod-shaped specimens
	ASTM D429-73	Rubber-to-metal bonding
	ASTM D1344-78	Cross-lap specimen specifically designed for glass substrates
Lap joints loaded in tension	BS 5350: Part C5: 1976	Single- or double-lap joint test
	ASTM D1002-72	Basic metal-to-metal single-lap joint test
	ASTM D3528-76	Double-lap joint test
	ASTM D3162-73 and D3164-73	Specifically for polymeric substrates
	ASTM D2295-72	Single-lap joint test for metal-to-metal joints at elevated temperatures
	ASTM D2557-72	As above but at low temperatures
	ASTM D905, D906, D2259 D2339 and D3535-76	Specifically for wooden joints
	ASTM 03983-81	Thick substrates used; shear modulus and strength of adhesive determined
Peel joints	BS 5350: Part C9: 1978 and ASTM D3167-76	Floating-roller test
	BS 5350: Part C10: 1976 and BS 5350: Part C14: 1979	90° peel test
	BS 5350: Part C11: 1979 and ASTM D903-49	180° peel test
	BS 5350: Part C12: 1979 and ASTM D1876-72	"T" peel test for flexible-to-flexible assemblies
	ASTM D1781-76	Climbing drum test for skin–sandwich assemblies
	ASTM D429-73	Rubber-to-metal bonding
	ASTM D2558-69	Shoe-soling materials
Cleavage strength	ASTM D1062-72	
	ASTM D3433-75	Parallel- or tapered-double-cantilever-beam joint for determining the adhesive fracture energy, $\mathcal{G}_{Ic}$
	ASTM D3807-79	Plastics-to-plastics joints
Block, shear, impact resistance	ASTM D950-78	
Disc shear strength in compression	ASTM D2182-72	
Creep resistance	BS 5350: Part C7: 1976	Various test geometries permitted
	ASTM D1780-72 and ASTM D2294-69	Single-lap joint loaded in tension employed
	ASTM D2293-69	Single-lap joint, having long overlap, and loaded in compression
Fatigue strength	ASTM D3166-73	Single-lap-joint loaded in tension employed
Environmental resistance	ASTM D2918-71	Subjected to stress, moisture and temperature; uses peel joint
	ASTM D2919-71	As above but uses single-lap shear joint loaded in tension
	ASTM D3762-79	As above but uses a wedge test
	ASTM D1151-72	Exposure to moisture and temperature
	ASTM D1183-70	Exposure to cyclic laboratory ageing conditions

TABLE III (*Continued*) ...

Test	Standard	Comments
	ASTM D904-57	Exposure to artificial and natural light
	ASTM D896-66	Exposure to chemical reagents
	ASTM D3632-77	Exposure of oxygen
	ASTM D1828-70	Natural weathering
	ASTM D1879-70	Exposure to high-energy irradiation
Pressure-sensitive tack	ASTM D2979-11	Inverted probe test
	ASTM D3121-73	Rolling-ball test
Flexural strength of laminated assemblies	ASTM D1184-69	
Torque strength	ASTM E229-70	For determining pure-shear strength and shear modulus of structural adhesives
	ASTM D3658-78	Specifically for ultra-violet light-cured glass–metal joints

(see Section 3.4.1. of Part 1 [1]). The data is shown in Fig. 12 and, as may be seen, the value of σ_b for the joints containing a thin adhesive layer is always greater than that for those having a thick layer, but their relationship to the cohesive tensile strength of the elastomeric adhesive is complex. Gent analysed these results using a fracture-mechanics approach and proposed that the total strain energy density, U_i, in the edge regions, where failure initiated, is given by the sum of the tensile and shear contributions,

$$U_i = \tfrac{1}{2}E_a e^2(1 + 3n^2r^2/t^2), \quad (39)$$

where e is the tensile strain and n is the stress-concentration of the edge geometry. The corresponding average tensile stress is obtained from the effective value E'_a of Young's modulus for cylinders bonded with a thin elastomeric layer (i.e., $\nu_a \to 0.5$)

$$\sigma = E'_a e = E_a e(1 + r^2/2t^2). \quad (40)$$

Hence, substituting for e from Equation 40 into

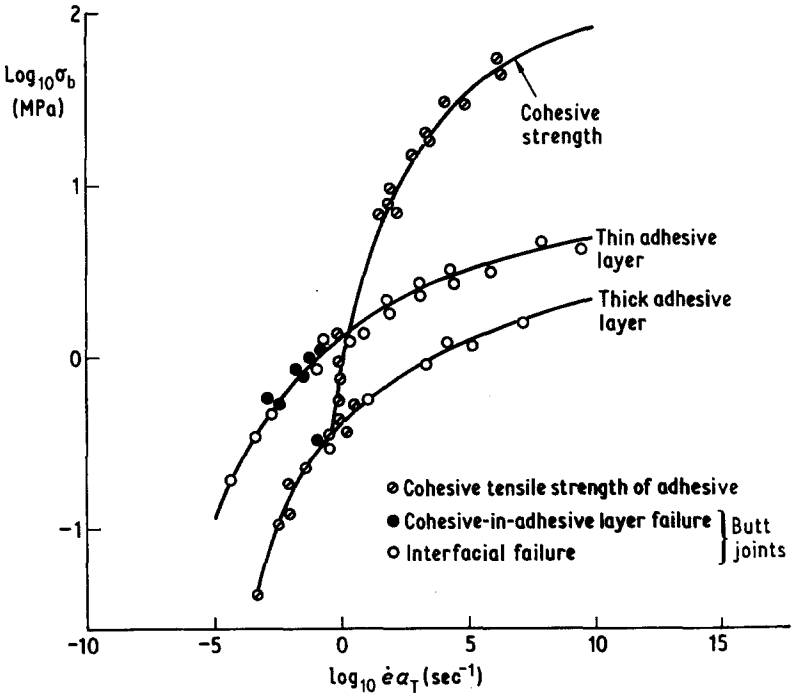

Figure 12 Cohesive and adhesive tensile failure stresses plotted against effective rate of extension, $\dot{e}a_T$, at 23° C (styrene–butadiene-rubber adhesive bonding polyethyleneterephthalate substrates), after Gent [192].

Equation 39, gives the adhesive fracture stress, σ_b, necessary to develop a critical strain energy, U_i, in the edge regions

$$\sigma_b = (2E_a U_i)^{1/2}(1 + r^2/2t^2)(1 + 3n^2r^2/t^2)^{-1/2}. \quad (41)$$

Thus, for a constant flaw size, when the radius r, is much larger than the thickness, t, of the adhesive layer, Equation 41 yields an inverse proportionality between the breaking stress, σ_b, and t. When the radius, r, is much smaller than t the value of σ_b is predicted to be independent of t. This general form of dependence is indeed commonly observed. Further, the above analysis shows that it arises from two competing effects: the greater stiffness of the test-pieces, necessitating a greater average tensile stress to achieve the same level of strain energy, and the increased concentration of shear strain, and hence strain energy, in the edge regions of thinner test-pieces causing failure at lower mean stresses than would otherwise be required. These features also assist in explaining the relationship between adhesive joint strength and cohesive strength of the elastomer. At relatively high rates of test and at low temperatures (i.e., high $\dot{e}a_T$ values) the elastomer becomes harder and stronger and eventually responds like a glassy solid. Under these conditions the cohesive strength is much greater than the joint strength and this may be partly ascribed to high stress concentrations in the joint. At low rates of extension and high temperatures the material deforms in a ductile manner and under these conditions the adhesive strength is similar or even slightly greater than the cohesive strength.

Hilton and Gupta [93] were concerned with structural adhesive joints consisting of an epoxy adhesive bonding aluminium-alloy substrate. They employed the stress-intensity factor approach and noted that Arin and Erdogan [105] had shown that the geometry factor, Q, in Equation 22 is a function of the ratio t/r for cracks in the mid-plane of the adhesive layer. As the adhesive layer decreases in thickness then the value of Q falls. Hence, for a given stress, σ, and flaw size, a, then the value of the stress-intensity factor, K_I, decreases as t decreases and is lower for the epoxy as a thin adhesive layer than as bulk material, albeit only marginally for very small flaw sizes. Since joint failure occurs when $K_I \geqslant K_{Ic}$, then, assuming that the fracture toughness, K_{Ic}, is independent of t, the adhesive joint strength will increase as t decreases.

However, the results of Adams and Coppendale [194] suggests a more complex situation. They examined a range of epoxy adhesives bonding aluminium-alloy substrates both theoretically and experimentally. They showed that the measured stress–strain behaviour of a butt joint is dependent upon the triaxial stress state induced in the adhesive by the restraint of the substrates, as discussed for rubbery adhesives above and in detail in Section 2.1. This causes a butt joint to yield at a stress which is greater then the uniaxial yield stress of the adhesive. Conversely, the presence of stress concentrations can cause a butt joint containing a relatively brittle adhesive to fail at a lower tensile stress than the failure stress of a bulk specimen tested in uniaxial tension. Therefore, Adams and Coppendale concluded that the relationship between the strength of a butt joint and that of a bulk specimen of the adhesive depended upon the ductility of the adhesive.

4.2.2. Lap joints

As predicted in Sections 2.2 and 2.3, for an essentially elastic adhesive the breaking load, F_b, increases up to an approximately constant value and the average applied stress, τ_b, at failure decreases as the overlap-length, l of a lap-joint is increased. This is illustrated in Fig. 13. However, if too short an overlap is employed high stresses will exist in the centre of the overlap upon loading and thus make the joint more susceptible to creep and environmental attack. The overlap should

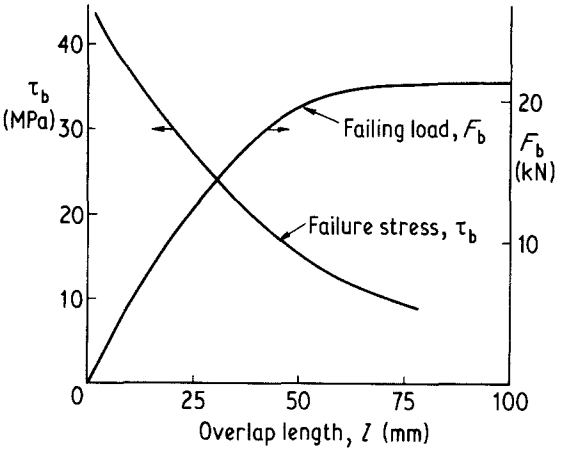

Figure 13 Failing load, F_b, and stress, τ_b, of single-overlap joint of modified-phenolic–aluminium-alloy as a function of overlap-length, l, after [31, 195].

therefore be sufficiently long to ensure these stresses are elastic in nature and low in magnitude. Further, if a ductile adhesive is used then a relatively long overlap (e.g., $l:d$ of about 80:1) will reduce [8] the eccentricity of the load path, and hence the tearing stresses, σ_{yy}, and so the breaking load F_b will continue to rise somewhat with increasing l. Increasing the thickness of the substrates results in a lower shear stress concentration but may increase the tensile, or tearing, stress, σ_{yy} [26]. Thus, increasing the thickness of the substrates results in higher joint strengths, up to a certain limit.

The theoretical analyses outlined in Sections 2.2 and 2.3 predict that the breaking stress, τ_b, of lap joints will increase as the thickness, t, of the adhesive layer increases. Generally, if all other joint parameters are held constant the value of τ_b is predicted to be proportional to the reciprocal of the square-root of the thickness, t, provided the thickness is relatively small. Fig. 14 taken from the work of Adams and Peppiatt [18] shows the predictions for three different analyses for an epoxy–aluminium-alloy single-lap joint and all suggest that the breaking load will increase as the value of t increases. However, the experimental results for the joints, in accord with other work [19, 189, 195–197], shows that the actual breaking load does not increase with increasing t and may even fall slightly.

4.2.3. Peel joints

In a recent review Gent and Hamed [198] considered the effects of thickness of the adhesive layer, thickness of the flexible substrate and peel angle.

In the case of adhesive thickness, t, they argued that the boundary cleavage stress, σ_a, (Equations 10 and 13) actually represents the mean tensile stress throughout the adhesive in the region of the debonding peel-front and not the much larger stress which acts at the line of interfacial separation. Thus, the degree of stress concentration at the line of separation will, in general, depend upon the thickness of the adhesive layer so that a larger mean stress will be necessary to bring about the same detachment stress in a thin layer than in a thicker one. Hence, the assumption in deriving Equation 10 of a constant value of σ_a, in the vicinity of the line of detachment, independent of t, is incorrect and they suggested that σ_a is inversely proportional to $t^{1/2}$. Therefore, both the stress analysis approach, Equation 13, and the energy-balance approach, Equation 30, predict that the peel force, F_b, should be independent of the thickness of the adhesive layer.

However, it is commonly observed [24, 47, 198–202] that the peel force, F_b, increases as the thickness, t, of the adhesive layer increases, and a typical relation is shown in Fig. 15. This behaviour, which is especially pronounced when the adhesive thickness is small, may be attributed to additional energy dissipation within the bulk of adhesive. It will be recalled that, as discussed in Part 1 (see Equation 26 of [1]) and in Section 3 of the present article, the energy dissipated by

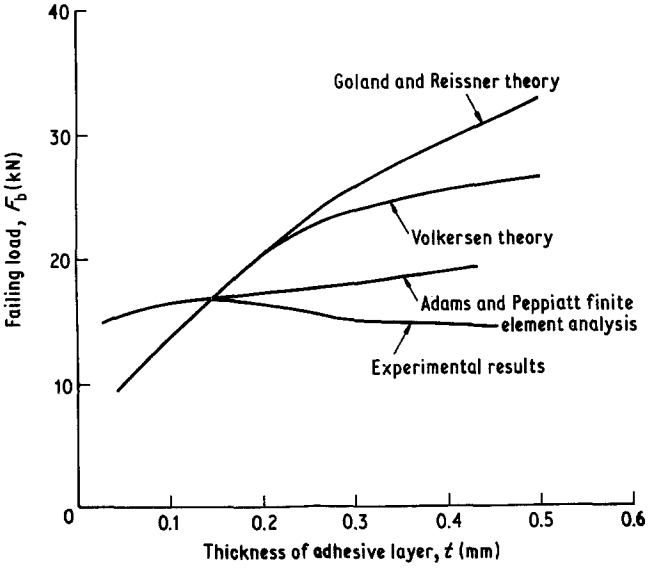

Figure 14 Influence of thickness, t, of adhesive layer upon experimental and theoretical failing loads of epoxy–aluminium-alloy single-lap joints, after Adams and Peppiatt [18].

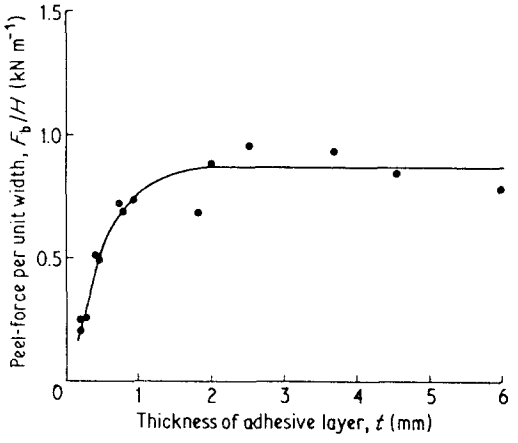

Figure 15 Relation between peel strength and thickness of adhesive layer for a polyethyleneterephthalate substrate detaching from a thermoplastic rubbery adhesive layer at a peel angle, α, of 180°, after Gent and Hamed [198].

viscoelastic and plastic deformation around the crack front usually dominates the measured energy to failure. Thus, as the adhesive thickness is increased in the peel test a large volume of adhesive is subjected to deformation per unit area of detachment so that the total work expended in peeling increases. However, at large thicknesses the energy dissipated during peeling then becomes independent of the overall thickness of the adhesive, since the dissipation process no longer involves the entire layer of adhesive. Adhesives capable of yielding and filamentation to large elongations thus give large peel strengths providing the interface is capable of withstanding sufficiently high stresses so that all the adhesive layer is brought into the yield region before detachment occurs.

Considering the effect of the thickness of the flexible, peeling substrate, Gent and Hamed [198] have suggested that for a sufficiently-long peeling strip the bending energy stays constant as peeling proceeds. Thus, provided the strip is perfectly elastic, no energy is dissipated within the substrate. However, if the level of adhesion is sufficiently high, or if the peeling strip is sufficiently thin, bending stresses may cause irreversible deformations of the substrate in the course of peeling and the peel force, F_b, will be augmented by the work expanded in plastic deformation of the substrate (Section 3.3.1). Experimentally it has been found [199, 203] that the relation between peel force and thickness of the peeling strip shows a maximum. This arises because, while a thin strip may undergo plastic yielding the total energy dissipated in this manner will be small. Hence, as the thickness of the peeling strip increases more energy is dissipated in yielding and F_b rises. However, at large thicknesses the backing will not experience sufficiently large bending stresses to cause yielding so that the peel force will decrease again back to the value obtained at zero thickness. Thus, the peel forces at both "zero" and large thickness of the substrate should be equal to the value of F_b in the absence of plastic yielding of the flexible substrate.

Both energy considerations and stress analysis lead to the conclusion that the peel force, F_b, should be inversely proportional to $(1 - \cos\alpha)$, where α is the peel angle. Many investigators [40–43, 50, 109–111, 203–206] have examined this dependence experimentally with conflicting results. In general, two principal discrepancies occur: at low peel angles, below about 30°, and at high peel angles, above about 150°. At low peel angles the measured peel force may be either less than [41] or greater than [204] that predicted, depending upon the adhesive–substrate combination. At high peel angles the value of F_b is usually greater than that expected. These discrepancies have been ascribed [198, 204] to energy dissipating processes which takes place to different extents at different peel angles.

4.2.4. Comparison of joint designs

Gent [86] has employed a fracture mechanics analysis to explain and predict joint strengths of a typical rubbery adhesive bonding relatively rigid substrates in tension, shear and peel. With the reasonable values of $E_a = 2$ MPa, $a = 0.1$ mm and $\mathscr{G}_c = 10\,\text{kJ m}^{-2}$ he predicted the dependence of the mean tensile breaking stress, σ_b, of butt joints upon the shape factor, r/t, of the adhesive layer from employing Equation 41, assuming $n = 3$. The results are shown in Table IV. Also given are the calculated peel strength, F_b/H, and shear strength, τ_b, obtained from Equation 30 assuming that the thickness of the adhesive layer is equal to or greater than the optimum value (see Fig. 14), and Equation 42 below, respectively,

$$\tau_b = n(2E_a\mathscr{G}_c/3\pi a)^{1/2}. \quad (42)$$

As may be seen, the shear strength, τ_b, is always less than the tensile strength, σ_b, and the latter rises to much greater values for thin adhesive layers. However, the relative values of σ_b, τ_b and

TABLE IV Strengths of rubber adhesive–rigid substrate joints tested in tension, shear and peel [86]

Joint geometry	Shape factor: radius/thickness, r/t	Strength
Butt joint	0.1	$\sigma_b = 4$ MPa
Butt joint	1	$\sigma_b = 2.5$ MPa
Butt joint	10	$\sigma_b = 11$ MPa
Butt joint	20	$\sigma_b = 21$ MPa
Shear joint	–	$\tau_b = 2$ MPa
Peel joint ($\alpha = 90°$)	–	$F_b/H = 10$ kN m^{-1}
See Fig. 9	–	$\mathscr{G}_c = 10$ kJ m^{-2}

F_b/H depend upon the values of E_a, the intrinsic flaw size, a, and local stress concentration effects. Ratios obtained with a particular adhesive–substrate combination will therefore not generally hold for others.

The physical properties of a typical modern structural adhesive examined in the form of both bulk specimens and adhesive joints is shown in Table V. The results in Table V clearly illustrate many of the aspects of joint design discussed above and demonstrate that the strength of an adhesive joint depends greatly upon the design employed. The higher 90° peel-strength found for the aluminium-alloy substrates reflects the extensive yielding which occurs as the aluminium-alloy is peeled away, while the steel substrate remains elastic. The importance of reducing the tensile stress, σ_{yy}, in double-lap joints consisting of cfrp substrates is evident. The single-lap joint strength is higher with the higher modulus, steel, substrates.

4.3. Effect of test temperature and rate

First, considering adhesives tested above their glass transition temperature, T_g, then it is well established [113–117, 192, 208–212] that the measured strengths of elastomeric adhesive joints obtained over a wide range of test temperatures and rates may be plotted to yield a single master curve when normalized to a reference temperature by means of the Williams–Landel–Ferry [213] rate–temperature equivalence for viscoelastic materials. Master curves for the adhesive fracture energies and tensile breaking stresses of rubbery adhesives are shown in Fig. 10 of Part 1 [1] and in Fig. 12 of the present paper. However, these relations are relatively simple resulting in a monotonic increase of either parameter with increasing rate and decreasing temperature but the relation for the peel strength of an uncross-linked

TABLE V Physical properties of rubber-toughened epoxy adhesive measured in bulk and in various adhesive joints [207]

Test	Substrates	Comments	Property
*Bulk properties**			
Flexure test	–	–	$E_a = 2.8$ GPa
	–	–	$\sigma_b = 74.5$ GPa
	–	–	$e_b = 2.7\%$
Glass transition, temperature, T_g	–	–	120° C
Adhesive joints†*			
Torsional shear	Aluminium-alloy	$t = 0.1$ mm	$\tau_b = 61$ MPa
Axially-loaded butt joints	Steel	$t = 0.5$ mm	$\sigma_b = 58$ MPa
Single-lap joint, loaded in tension	(i) Aluminium-alloy	$t = 0.5$ mm, $d = 1.6$ mm, $l = 12.7$ mm	$F_b = 9$ kN; $\tau_b = 28$ MPa
	(ii) Steel	As above	$F_b = 12.3$ kN; $\tau_b = 38$ MPa
Double-lap joint, loaded in tension	(i) Cfrp–steel	No taper; $l = 80$ mm	$F_b = 24$ kN; $\tau_b = 6.9$ MPa
	(ii) Cfrp–steel	Reverse taper; $l = 80$ mm	$F_b = 80$ kN; $\tau_b = 19.7$ MPa
Peel joints† 90° peel (floating-roller)	(i) Steel		$F_b/H = 0.6$ kN m^{-1}
	(ii) Aluminium-alloy		$F_b/H = 5$ kN m^{-1}
135° peel	Aluminium-alloy		$F_b/H = 4$ kN m^{-1}
Pre-cracked, tapered-double-cantilever beam	Steel		$\mathscr{G}_{Ic} = 0.9$ kJ m^{-2}
Pre-cracked, compact shear	Steel		$\mathscr{G}_{IIc} = 2.2$ kJ m^{-2}

* Tests conducted at 23° C and a moderate rate.

† All joints failed by cohesive fracture through the adhesive except for the cfrp–steel double-lap joints which failed in the cfrp substrate.

elastomeric adhesive may be extremely complex [210, 214]. Gent and Petrich [210] reported two main features for such a master curve: a sharp maximum occurring at low rates and high temperatures, which may in some instances be accompanied by a transition from cohesive-in-adhesive to interfacial failure, and a sharp decrease in peel strength at high rates and low temperatures. The former feature was shown to arise from a change in the deformation process in the adhesive from a liquid-like to a rubber-like response and Gent and Petrich proposed an approximate relation between peel strength and the tensile stress–strain behaviour of the bulk adhesive using a single empirically-determined parameter, namely the interfacial bond strength. The second effect was due to the transition from a rubber-like to glass-like response of the adhesive and to the exact peel geometry employed.

Second, considering adhesives tested largely below their glass transition temperature, Fig. 16 illustrates some typical results for various adhesive compositions. The epoxy–phenolic, polyimide and polybenzimadzole exhibit the best high-temperature strengths of those shown. In a recent review Cotter [215] concluded that the former formulations are available for long-term use to about 175° C and are capable of short excursions to temperatures as high as 250° C. The polyimide compositions may be used for very long times at 260° C and maintain a useful strength at 425° C for about 1 h. Polybenzimadazole adhesives have a higher temperature ceiling than polyimide formulations in inert atmospheres but are markedly susceptible to oxidative degradation above 260° C. The relationship between low-temperature performance and the structure and formulation of the adhesive have also been considered [217, 218]. Increasing the rate of loading structural adhesive joints is generally equivalent to decreasing the test temperature, as would be expected.

The creep and stress rupture of adhesive joints under static [167, 219–227] and dynamic [228–234] loadings have been the subject of many investigations. The failure behaviour of epoxy adhesives when subjected to a constant applied load is particularly intriguing. It has been reported [167] that some epoxy adhesive joints, tested in a tapered-double-cantilever-beam geometry, do not appear to suffer from static fatigue, even when stressed to a relatively high level. This arises because severe crack-tip blunting reduces the stress concentration at the crack tip to such an extent that the tip stress level [235, 236] necessary for crack extension is not attained and thus this mechanism forestalls static-fatigue failure. However, in compositions where the capacity for crack-tip blunting during the static fatigue test is limited, delayed failure is observed. Gledhill and Kinloch [227] have studied one such epoxy adhesive composition and a linear relationship was found to exist between the applied fracture energy, $\mathscr{G}_{Ic}$, and the logarithmic failure time, the failure time decreasing as the value of $\mathscr{G}_{Ic}$ was increased. The failure time

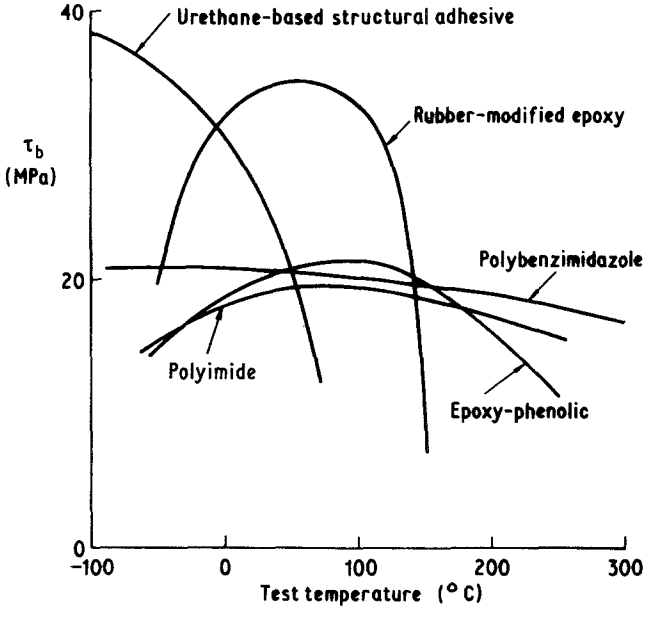

Figure 16 Typical strengths of single-lap joints loaded in tension using various structural adhesives as a function of test temperature, after [215, 216].

represented an incubation period: the crack was not observed to propagate until the very end of the experiment, at the instant of fracture, when it propagated very rapidly. From a fracture-mechanics analysis, the plastic-zone size at fracture, r_{Iyc}, and crack-opening displacement at fracture, δ_{tc}, may be related to the time-dependent fracture energy, $\mathcal{G}_{Ic}(t)$, and the time-dependent modulus, $E_a(t)$, by the relations

$$r_{Iyc} = \frac{1}{6\pi(1-\nu^2)e_y^2}\frac{\mathcal{G}_{Ic}(t)}{E_a(t)} \quad (43)$$

and

$$\delta_{tc} = \frac{1}{(1-\nu^2)e_y}\frac{\mathcal{G}_{Ic}(t)}{E_a(t)}, \quad (44)$$

where e_y is the yield strain and the first terms on the right-hand side of Equations 43 and 44 are approximately constant. Values of $\mathcal{G}_{Ic}(t)$ and corresponding values of $E_a(t)$ are plotted in Fig. 17 and yield a linear relation over the entire scale of about seven decades over which the static fatigue experiments were conducted. Thus, constant values of r_{Iyc} and δ_{tc} of 16 and 4.5 μm, respectively, therefore provided a unique failure criterion and, until these critical values are attained no crack extension was found to occur.

Bascom and Mostovoy [234] and Mostovoy and Ripling [237] have used a fracture-mechanics approach to study fatigue crack growth in rubber-toughened structural adhesives. They found that

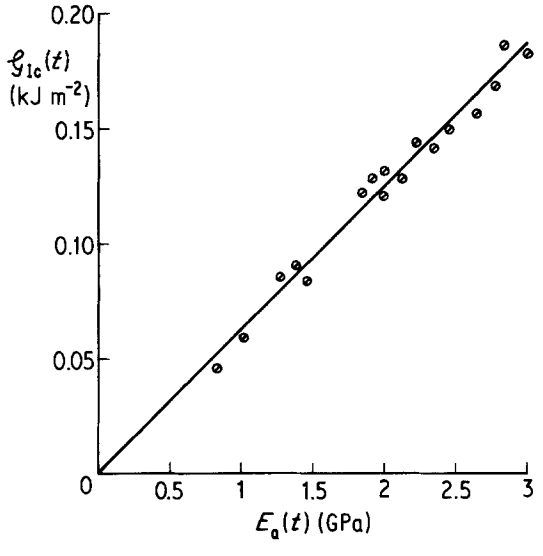

Figure 17 Applied adhesive fracture energy, $\mathcal{G}_{Ic}(t)$ as a function of corresponding modulus, $E_a(t)$ for static fatigue tests, after Gledhill and Kinloch [227].

such crack growth could be described by the Paris Equation [84]

$$\frac{da}{dN} = A\Delta\mathcal{G}_I^n, \quad (45)$$

where da/dN is the crack-growth per cycle and $\Delta\mathcal{G}_I$ is the applied adhesive fracture energy where

$$\Delta\mathcal{G}_I = \mathcal{G}_I(\text{maximum}) - \mathcal{G}_I(\text{minimum}) \quad (46)$$

and A and n are constants. Depending upon the adhesive formulation, A varied between about 10^{-14} to 10^{-16} and n varied between 2.8 and 4.0 (da/dN in m cycle^{-1} and $\mathcal{G}_I$ in J m^{-2}).

5. Environmental attack

5.1. Introduction

A serious limitation that has been encountered in the use of adhesives, especially for structural engineering applications, is the deleterious effect that moisture may have upon the strength of a bonded component [172, 174, 238–241]. Such effects are particularly pronounced when the component is also subjected to conditions of relatively high stress and temperature. The mechanisms and kinetics of such environmental failure will be first discussed, followed by a consideration of the methods which have been developed to increase the service-life of adhesive joints

5.2. Mechanisms of failure

5.2.1. Stability of the adhesive

It is an obvious statement that if the service environment physically or chemically attacks the adhesive to any significant extent then the joint may well be appreciably weakened. However, assuming a degree of common-sense has been exercised in adhesive selection, then loss of strength in the adhesive is not usually a major mechanism of attack in aqueous environments. This is evident from the frequent observation that, while the locus of failure of well prepared joints is invariably by cohesive fracture in the adhesive layer, after environmental attack it is usually via "apparent" interfacial failure between the adhesive (or primer) and substrate.

5.2.2. Stability of the interface

The above observation highlights the importance of the interface when considering environmental failure mechanisms. The thermodynamic work of adhesion, W_A, required to separate unit area of two phases forming an interface may be related to

the surface free energies by the Dupre equation (see [1]). In the absence of chemisorption, interdiffusion and mechanical interlocking, the reversible work of adhesion, W_A, in an inert medium may be expressed by

$$W_A = \gamma_a + \gamma_b - \gamma_{ab}, \quad (47)$$

where γ_a and γ_b are the surface energies of the two phases and γ_{ab} is the interfacial free energy. In the presence of a liquid (denoted by the subscript L), the work of adhesion, W_{AL}, is

$$W_{AL} = \gamma_{aL} + \gamma_{bL} - \gamma_{ab}. \quad (48)$$

For an adhesive–substrate interface the work of adhesion, W_A, in an inert atmosphere, for example dry air, usually has a positive value, indicating thermodynamic stability of the interface. However, in the presence of a liquid the thermodynamic work of adhesion, W_{AL}, may well have a negative value indicating the interface is now unstable and will dissociate. Thus, calculation of the terms W_A and W_{AL} may enable the environmental stability of the interface to be predicted.

The values of W_A and W_{AL} may be calculated [170, 242]

$$W_A = 2(\gamma_a^D \gamma_b^D)^{1/2} + 2(\gamma_a^P \gamma_b^P)^{1/2} \quad (49)$$

$$W_{AL} = 2[\gamma_L - (\gamma_a^D \gamma_L^D)^{1/2} - (\gamma_a^P \gamma_L^P)^{1/2} - (\gamma_b^D \gamma_L^D)^{1/2} - (\gamma_b^P \gamma_L^P)^{1/2}] \quad (50)$$

where γ^D and γ^P are the dispersion and polar force components, respectively, of the surface free energy, γ.

Some examples of values of W_A and W_{AL} are shown in Table VI and the generality of this concept is illustrated by reference to environments other than water.

For those interfaces where there is a change from positive to negative work-of-adhesion then this provides a driving force for the displacement of adhesive on the substrate surface by the liquid. It is therefore to be expected that, if the joint is subjected to such an environment there will be a progressive encroachment into the joint of debonded interface. This will have the effect of progressively reducing the joint strength and also of progressively changing the locus of failure to interfacial between adhesive and substrate. This is exactly what has been observed in practice [242, 245]. However, it should be recalled that the measured adhesive failure energies required for the range of crack growth rates normally encountered are much higher than the values of the thermodynamic work of adhesion shown in Table VI [87, 168]. This is because, under an applied load, mechanical strain-energy is available to assist environmental cracking or debonding and this is reflected in inelastic energy dissipative processes,

TABLE VI Values of W_A and W_{AL} for various interfaces and environments

Interface	Work of adhesion ($mJ\ m^{-2}$)		Evidence of interfacial bonding after immersion of unstressed joints	Reference number
	Inert medium: W_A	In liquid medium: W_{AL}		
Epoxy adhesive–ferric oxide (mild-steel)	291	Ethanol: 22	No	[242]
		Formamide: −166	Yes	[242]
		Water: −255	Yes	[242]
Epoxy adhesive–aluminium-oxide	232	Water: −137	Yes	[157]
Epoxy adhesive–silica	178	Water: −57	Yes	[157]
Epoxy adhesive–carbon-fibre-reinforced plastic	88 to 90	Water: 22 to 44	No	[243]
Vinylidene chloride-methylacrylate co-polymer–polypropylene	88	Water: 37	No	[244]
		Sodium *n*-octyl sulphate (3.5% wt % solution) 1.4	No	
		Sodium *n*-dodecyl sulphate (0.5% wt % solution) −0.9	Yes	
		Sodium *n*-hexadecyl sulphate (0.05% wt % solution) −0.8	Yes	

e.g. plastic flow, occurring in regions of the adhesive around the crack tip. The values of W_A and W_{AL} do not allow for any such processes.

In those instances where W_{AL} is not negative but $W_A > W_{AL} \geqslant 0$ then the input of additional work is a necessary requisite for joint failure. However, as might be expected, the measured adhesive failure energy for interfacial crack growth is now reduced by the presence of the liquid [87, 144, 246]. Gent and Schultz [246] measured the failure energy of a cross-linked styrene–butadiene rubber adhering to a polyethylene-terephthalate substrate and conducted experiments in air and in an alcohol–water series of liquids. They found that the failure energy was reduced from the latter experiments and that the reduction factor was in good agreement with that predicted from simple thermodynamic considerations, similar to those described above.

Finally, it should be noted that the thermodynamics as stated in Equations 47 to 50 take no account of interfacial adhesion forces arising from primary bonds or mechanical interlocking. Further, they provide no information on the expected service-life of joints upon being stressed in hostile environments. For this data the thermodynamic analysis needs to be combined with either a stress-biased activated rate theory, as developed by Zhurkov and co-workers [247, 248], and used in joint fracture studies by Levi *et al.* [249], or a continuum fracture-mechanics approach [173, 250].

5.2.3. Stability of the substrate

Obviously, environmental attack on the substrate material may well cause a loss in joint strength but, if "gross" effects are considered, then this is not usually a major mechanism of environmental failure. For example, corrosion of the surface of a metallic substrate is often a post-failure phenomenon, occurring after the displacement of adhesive on the metal oxide by water [242]. Only in special curcumstances, for example with clad aluminium-alloys or in a salt-water environment, is gross corrosion of the substrate an important failure mechanism.

The potential problem with clad aluminium-alloy is of particular interest and has been studied in detail by Riel [251]. With clad aluminium-alloys the electrode potential of the cladding is generally higher than that of the base alloy. This choice is deliberate in that the clad material is selected to be anodic with respect to the base alloy so that, in a corrosive environment, the cladding will be consumed, thus protecting the base alloy. This mechanism is very effective in protecting the structure from surface corrosion, such as pitting, since pitting of clad alloy is less likely to occur due to the nature of the alloy and where pits do form and penetrate the clad surface its anodic nature will cause the pit to grow laterally once the base alloy is reached, rather than penetrating into the base alloys as is seen with unclad alloy. However, while this mechanism of corrosion protection inhibition may be effective for exposed aluminium-alloy structures, if one considers the mechanisms whereby clad aluminium-alloy achieves its corrosion resistance then the clad layer may be actually undesirable in the context of adhesive bonding. A galvanic cell may be established between cladding and base alloy with the progressive destruction of the interfacial regions. In the United States aerospace industry the current trend is away from adhesive bonding to clad aluminium-alloys [174, 252, 253]; however, where unclad alloys are bonded and used in areas exposed to corrosive environments any non-bonded, exterior surface must be protected by appropriate means in order to limit surface corrosion.

With regard to more subtle changes induced in the nature of the surface of the substrate by an active environment, then Noland [254] has reported that the oxide produced on aluminium-alloys by a chromic–sulphuric acid etch, a common pre-treatment technique in the aerospace industry, is unstable in the presence of moisture. He has postulated that the oxide changes to a weaker, gelatinous type which is hydrated and is termed "gelatinous-boehmite". His evidence for the change in oxide structure comes from X-ray photoelectron spectroscopy analysis of the oxide surface before and after ageing and Fig. 18 shows that a change in binding energy is observed for the aluminium 2p-peak position, indicating a change in oxide structure. Noland also examined epoxy–aluminium-alloy joints after exposure to hot, humid conditions and reported that, although from a visual inspection apparent interfacial failure had occurred, in fact the locus of failure was in the mechanically-weak gelatinous-boehmite oxide layer. Recent work [255] using electron diffraction and scanning transmission electron miscroscopy has essentially confirmed the conclusions of this

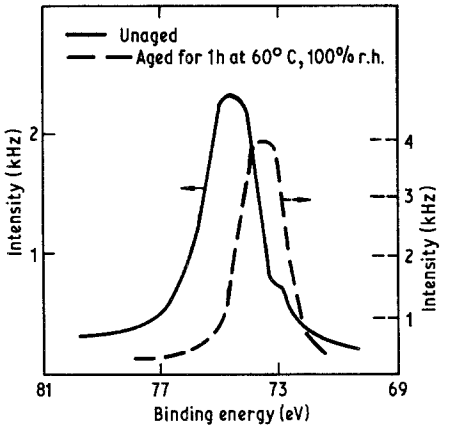

Figure 18 X-ray photoelectron spectroscopy analysis of chromic–sulphuric acid etched aluminium-alloy surface (Al 2p-peak) before and after ageing, after Noland [254].

earlier study. The original oxide formed by the pre-treatment was found to be largely amorphous but, upon exposure to moisture, became hydrated and possessed a crystalline, pseudo-boehmite (i.e., a material containing somewhat more water than perfectly-crystallized boehmite) structure. This hydrated oxide could be readily distinguished by its distinctive morphology which consisted of irregular-shaped platelets; which the author dubbed a "cornflake structure". This structure was, however, only loosely bound to the underlying oxide and thus represented a weak boundary layer (see [1]), but one which was actually formed *in situ* in the joint.

However, the reason why certain pre-treatments coupled with specific grades of aluminium-alloy result in adhesive joints possessing vastly different resistances to environmental attack by water has yet to be resolved in detail. Sun *et al.* [256] have employed Auger spectroscopy to characterize acid-etched aluminium alloys and have suggested that it is the accumulation of certain elements, such as copper and magnesium at the oxide–metal interface or in the oxide layer which are detrimental to oxide stability and joint durability. Kinloch and Smart [257], using X-ray photoelectron spectroscopy, have also recently identified a correlation between high magnesium content in the oxide layer and poor joint durability. These conclusions are qualitatively supported by observations from other sources [256]. For example, Minford [258] has reported extremely poor bond durability when bonding vapour-degreased 6061-T3 aluminium-alloy while Smith and Martinsen [259] have reported that this alloy has a magnesium-rich surface.

5.3. Kinetics of failure

Several workers [173, 242, 260–266] have shown that the kinetics of the environmental failure mechanism may be governed by the rate of diffusion of water into the joint. Fortunately, water up-take by cross-linked adhesives often behaves according to Fick's law and thus, from measuring the diffusion constant, using bulk adhesive film samples, the water concentration profile within the joint as a function of geometry, temperature and water activity may be predicted [173, 260, 265, 266]. Comyn and co-workers [260, 267] and Althof [265, 266] have shown that these predictions are reasonably accurate, certainly around the periphery of the joint where the initial de-bonding occurs.

Comyn and co-workers [260, 261, 263, 264] have also demonstrated that a linear relationship often exists between loss of joint strength and total water content of the adhesive layer. Recently Gledhill *et al.* [173] have undertaken quantitative predictions for the durability of unstressed butt joints consisting of mild-steel substrates bonded with a simple epoxide adhesive. First, from diffusion data for the adhesive, concentration profiles for water ingressing into the adhesive joint were calculated as a function of time and temperature. For this joint, environmental attack occurs by truly interfacial failure and, in the absence of an applied stress, the kinetics are governed solely by the rate of water diffusion. Second, therefore, by assigning a constant, critical water concentration for de-bonding, the interfacial environmental crack-length, a, as a function of the time spent in the water at a given temperature, was deduced. Third, this crack-length was combined with the independently-measured values of $\mathcal{G}_{Ic}$ and E_a of the adhesive and, via Equations 23 and 25, used to predict the failure stress expected when the joint was subsequently removed from the environment and fractured. The predictions, over a wide range of times and temperatures, were in excellent agreement with the experimentally-determined values.

5.4. Effects of stress

The rate of loss of strength will be faster if a tensile or shear stress is present, albeit an externally

applied stress or internal stresses induced by adhesive shrinkage (incurred during cure) or by adhesive swelling (due to water uptake) [70, 87, 168, 172, 174, 240, 250, 252, 268]. Such stresses render primary and secondary bonds more susceptible to environmental attack by lowering the free energy barrier that must be crossed if the bond is to change from an unbroken to a broken state, i.e., lower the activation energy for, and so increase the rate of, bond rupture. Stress also probably increases the rate of diffusion of the ingressing medium. On the positive side, plasticization of the adhesive may diminish stresses by stress relaxation and crack blunting mechanisms. Indeed, crack-tip blunting may actually cause the apparent toughness of the adhesive to increase, and such an effect has been reported after short exposure times insufficient for significant interfacial attack [144, 147, 168].

5.5. Increasing joint durability

The deleterious effect of water on the joint strength and post-failure corrosion of the substrate could be avoided if the integrity of the interfacial regions could be maintained. Thus, either water must be prevented from reaching the interface in sufficient concentration to cause damage or the intrinsic durability of the interface must be increased.

5.5.1. Decreasing water permeation

All organic polymers are permeable to water and values of permeability coefficients and diffusion constants may be found in the literature [172, 260, 269]. However, structural adhesives are usually based upon epoxy or phenolic polymers and these materials are already at the low end of the spectrum of such values. Thus, whilst there is undoubtedly room for improvement the other properties of any adhesive, such as wetting–adhesion characteristics, processability, toughness, cost, etc. must be balanced against the need for low water permeability.

A second approach has been to use sealants (which are usually based upon organic polymers) to coat the edges of the exposed joint. However, while this will obviously slow down water penetration it is often not possible to apply a thick enough layer to be very effective and this approach has other disadvantages such as adding an extra operation and cost to the bonding process.

5.5.2. Establishing primary interfacial bonding

Considering first only secondary-force interactions across the interface then the relations derived in Section 5.2.2. may be used to predict, for a given substrate and liquid environment, the required values of γ^D and γ^P of the adhesive if adhesive–substrate interface stability is to be maintained in the presence of the environment. Such results are shown graphically in Fig. 19 for a polyethyleneterephthalate substrate and a mild-steel substrate (Fe_2O_3 oxide surface) with, in both cases, water as the hostile environment. See also Table VII. Values of γ^D and γ^P of some adhesives were given in Table I of [1]; for example, considering a styrene–butadiene rubbery adhesive,

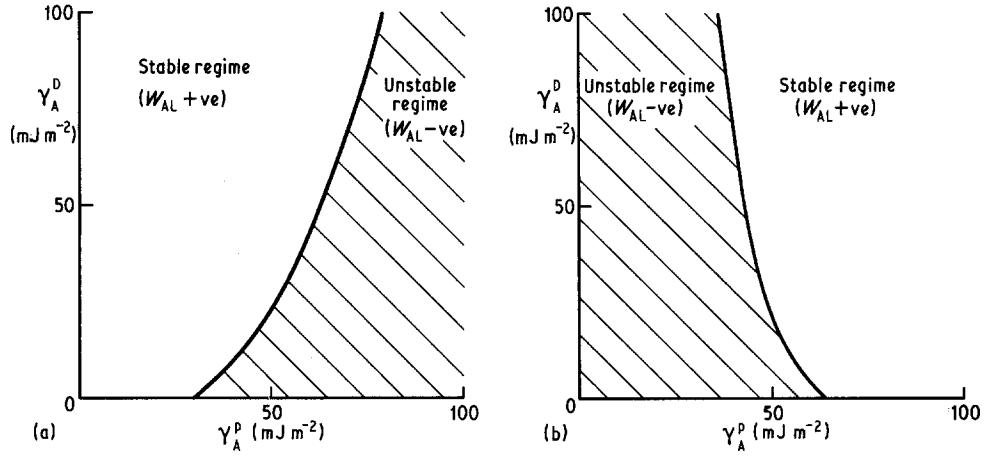

Figure 19 Predictions of interface stability for (a) polyethyleneterephthalate substrate and water environment and (b) Fe_2O_3 substrate and water environment as a function of γ_A^D and γ_A^P values of potential adhesives. See also Table VII.

TABLE VII Predictions of interface stability for various substrates and environments

Substrate/Environment	γ^D (mJ m^{-2})	γ^P (mJ m^{-2})	γ (mJ m^{-2})
Substrate : Polyethyleneterephthalate	41.8	3.3	45.1
Substrate : Fe_2O_3	107	1250	1357
Environment : Water	22.0	50.2	72.2

the values are 27.8 and 1.3 mJ m^{-2}, respectively, and for an amine-cured epoxy-resin adhesive the values are 41.2 and 5.0 mJ m^{-2}, respectively. Hence, it is evident that these (and most other) adhesives will form an environmentally water-stable interface with the polyethyleneterephthalate substrate but an unstable interface with mild-steel. Indeed, the thermodynamics indicate that if only secondary forces are acting across the interface, water will virtually always desorb an organic adhesive from a metal oxide surface. Hence, for such interfaces stronger forces must be forged which are resistant to rupture by water.

The establishment of primary, interfacial bonds between epoxy adhesives and metal oxide surfaces via an organo-metallic primer and the evidence [270, 271] for such a reaction was discussed in Part 1 [1]. The improvement in joint durability that can be achieved is shown in Fig. 20. It would be of considerable interest if the contribution from interfacial primary bonds to the intrinsic stability of the interface could be quantified, however, without a more detailed knowledge of the type of reactions, and their extent, it is at present impossible to calculate their contribution exactly. Nevertheless, an approximate indication may be obtained by taking the interfacial, chemical bond energy as 250 kJ mol^{-1} (from Table III in Part 1 [1]) and, assuming a coverage of 0.25 nm^2 per adsorbed site. This yields an intrinsic work of adhesion of + 1650 kJ m^{-2} and from energetic considerations it would be unlikely that water would readily displace such a chemisorbed primer layer. More basic information on the interfacial forces and reaction mechanisms is required before more definitive calculations and predictions can be undertaken.

Finally, the presence of interfacial, covalent bonds has been suggested [272] to explain why phenolic-based adhesives and primers generally impart very good durability characteristics [252]. Basically, the reaction conditions required to cure these materials are considered to be precisely those which give the maximum probability of forming ether linkages between an oxide surface and the resin. However, the existence of such an interfacial bond has yet to be positively established, although some evidence [273] from inelastic tunnelling spectroscopy does indicate its formation. Such a

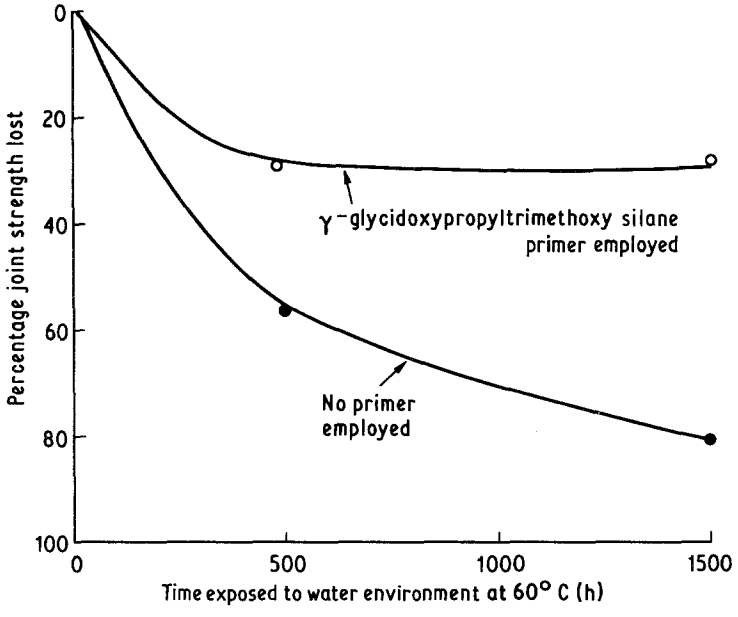

Figure 20 Increased durability of epoxy adhesive–mild-steel joints achieved using an organo-metallic primer, after Gettings and Kinloch [270].

bond might be expected to be susceptible to hydrolysis in water because of its strongly ionic character.

5.5.3. Substrate stability

Stability of the substrate surface to which the adhesive is attached is an obvious requirement for ensuring durable joints. This emphasizes the important role that the selection of pre-treatment technique, prior to adhesive bonding, assumes in ensuring adequate service-life of the bonded joint.

In the case of aluminium-alloys, workers [174, 274, 275] at the Boeing Commercial Airplane Company have recently developed a new surface pre-treatment method based upon phosphoric-acid anodizing. This method results in improved joint durability, although the exact mechanism underlying this improvement has yet to be conclusively established. Noland [255] employed X-ray photoelectron spectroscopy and the results indicated that the oxide formed was more stable than that formed by a chromic–sulphuric acid-etch method to the presence of moisture. Also, Bascom [240] has recently drawn attention to the thick, porous oxide structure [174, 276] produced by this pre-treatment. Penetration would result in a resin–metal oxide composite interface region that may contribute significantly to joint durability, since failure through the oxide would involve plastic and viscoelastic deformation of the ligaments of the adhesive (or primer) (see Section 3.1 of [1]). Also, in such a process, mechanical interlocking may contribute significantly to the intrinsic adhesion [240, 276, 277] and thus invalidate the thermodynamic work of adhesion as a sole criteria for interface stability. Hence, it appears that in certain circumstances the oxide must possess both a resistance to attack by water and the "correct" microstructure for maximum joint durability.

However, it is not, at present, possible to define in detail the exact surface chemical and physical parameters which are important for producing an oxide layer which will impart good environmental resistance to an adhesive joint.

6. Concluding remarks

The two papers which form this review have attempted to discuss critically various aspects of adhesion science which are relevant to the adhesive joining of materials with the aim of outlining the current philosophies and relating them, where possible, to the practice of adhesive bonding. It is evident that there are many areas, especially those concerned with the mechanisms of adhesion and joint failure, where the knowledge is inadequate. Until such aspects are more completely understood the full potential of adhesives as a means of joining materials will not be realised.

Acknowledgements

The author would like to thank Dr R. D. Adams of Bristol University for many helpful comments during the preparation of this paper. This Review is published by the permission of Copyright © Controller HMSO, London, 1981.

References

1. A. J. KINLOCH, *J. Mater. Sci.* **15** (1980) 2141.
2. R. S. ALWAR and Y. R. NAGARAJA, *J. Adhesion* 7 (1976) 279.
3. R. D. ADAMS, J. COPPENDALE and N. A. PEPPIATT, *J. Strain Anal.* **13** (1978) 1.
4. E. W. KUENZI and G. H. STEVENS, U.S. Forest Products Laboratory, Report Number FPL-011 (1963).
5. A. N. GENT and P. B. LINDLEY, *Proc. Roy. Soc.* **A249** (1958) 195.
6. *Idem, Proc. Inst. Mech. Eng.* **173** (1959) 111.
7. B. P. HOLOWNIA, *J. Strain Anal.* 7 (1972) 236.
8. L. J. HART-SMITH, in "Developments in Adhesives-2" edited by A. J. Kinloch (Applied Science Publishers, London, 1981) p. 1.
9. R. D. ADAMS, in "Developments in Adhesives-2" edited by A. J. Kinloch (Applied Science Publishers, London, 1981) p. 45.
10. N. L. HARRISON and W. J. HARRISON, *J. Adhesion* **3** (1972) 195.
11. O. VOLKERSEN, *Luftfahrtforsch* **15** (1938) 41.
12. M. GOLAND and E. REISSNER, *J. Appl. Mech.* **2** (1944) A-17.
13. C. MYLONAS, *Proc. Soc. Exp. Stress Anal.* **12** (1954) 129.
14. I. SNEDDON, in "Adhesion" edited by D. D. Eley (Oxford University Press, London, 1961) p. 207.
15. L. GREENWOOD, in "Aspects of Adhesion-5" edited by D. J. Alner (University of London Press, London, 1970) p. 40.
16. R. D. ADAMS, S. H. CHAMBERS, P. J. A. DEL STROTHER and N. A. PEPPIATT, *J. Strain Anal.* **8** (1973) 52.
17. R. D. ADAMS and N. A. PEPPIATT, *ibid.* 8 (1973) 134.
18. R. D. ADAMS and N. A. PEPPIATT, *ibid.* 9 (1974) 185.
19. R. D. ADAMS, J. COPPENDALE and N. A. PEPPIATT, in "Adhesion-2" edited by K. W. Allen (Applied Science Publishers, London, 1978) p. 105.
20. W. J. RENTON and J. R. VINSON, *J. Adhesion* 7 (1975) 175.
21. *Idem, Eng. Fract. Mechs.* 7 (1975) 175.
22. *Idem, J. Appl. Mech.* **44** (1977) 101.

23. D. J. ALLMAN, *Mechs. Appl. Maths.* **30** (1977) 415.
24. D. W. CHERRY and N. L. HARRISON, *J. Adhesion* **2** (1970) 125.
25. L. J. HART-SMITH, National Aeronautics and Space Administration, Washington D.C., Report Number CR-2218, 1974.
26. *Idem,* Douglas Aircraft Co., Long Beach, CA, Report Number 6059A, 1972.
27. *Idem,* Douglas Aircraft Co., Long Beach, CA, Report Number 6224, 1974.
28. *Idem,* Douglas Aircraft Co., Long Beach, CA, Report Number 6707, 1978.
29. *Idem,* Douglas Aircraft Co., Long Beach, CA, Report Number 6922, 1980.
30. P. J. GRANT, "Jointing in Fibre Reinforced Plastics" (IPC, Guildford, 1978) p. 41.
31. C. MYLONAS and N. A. DE BRUYNE, in "Adhesion and Adhesives" edited by W. A. De Bruyne and R. Houwink (Elsevier, Amsterdam, New York and Oxford, 1951) p. 91.
32. O. ISHAI, D. PERETZ and S. GALI, *Expt. Mechs.* **17** (1977) 265.
33. R. P. PENNING, Engineering Sciences Data Unit, London, Report Number 7 8042, 1978.
34. O. VOLKERSEN, *Const. Met.* **4** (1965) 3.
35. F. ERDOGAN and M. RATNANI, *J. Adhesion* **5** (1971) 378.
36. F. THAMM, *ibid.* **7** (1976) 301.
37. B. W. CHERRY and N. L. HARRISON, *ibid.* **2** (1970) 125.
38. M. D. WRIGHT, *Composites* **9** (1978) 259.
39. G. N. SAGE, in "Adhesion-3" edited by K. W. Allen (Applied Science Publishers, London, 1979) p. 123.
40. D. H. KAELBLE, *Trans. Soc. Rheol.* **3** (1959) 161.
41. *Idem, ibid.* **4** (1960) 45.
42. *Idem, ibid.* **9** (1965) 135.
43. D. H. KAELBLE and C. L. HO, *ibid.* **18** (1974) 219.
44. J. J. BIKERMAN, *J. Appl. Phys.* **28** (1957) 1484.
45. Y. INOUE and Y. KOBATAKE, *Appl. Sci. Res.* **A8** (1959) 321.
46. J. L. GARDON, *J. Appl. Polymer Sci.* **7** (1963) 625.
47. *Idem, ibid.* **7** (1963) 643.
48. G. J. SPIES, *Aircraft Eng.* **30** March (1953) 2.
49. C. JOUWERSMA, *J. Polymer Sci.* **45** (1960) 253.
50. C. MYLONAS, Proceedings of the 4th International Congress on Rheology, Providence, USA, 1963, Part 2 (Wiley Interscience, New York, 1965) p. 423.
51. J. J. BIKERMAN, "The Science of Adhesive Joints" (Academic Press, New York, 1968) p. 243.
52. W. C. WAKE, "Adhesion and the Formulation of Adhesives" (Applied Science Publishers, London, 1976) p. 121.
53. A. W. GENT and G. R. HAMED, *J. Adhesion* **7** (1975) 91.
54. A. CROCOMBE and R. D. ADAMS, "Adhesion and Adhesives: Science, Technology and Applications" (Plastics and Rubber Institute, London, 1980) p. 10.1.
55. R. D. ADAMS and A. CROCOMBE, *J. Adhesion* **12** (1981) 127.
56. R. L. LUBKIN and E. REISSNER, *Trans. ASME* **78** (1956) 1213.
57. N. M. KUKOVYAKIN and I. A. SKORYI, *Russ. Eng. J.* **52**(4) (1972) 40.
58. L. P. TEREKHOVA and I. A. SKORYI, *Strength Mater.* **4** (1973) 1271.
59. R. D. ADAMS and N. A. PEPPIATT, *J. Adhesion* **9** (1977) 1.
60. Y. R. NAGARAJA and R. S. ALWAR, *ibid.* **10** (1979) 97.
61. H. FOULKES, J. SHIELDS and W. C. WAKE, *ibid.* **2** (1970) 254.
62. R. W. BRYANT and W. A. DUKES, *Brit. J. Appl. Phys.* **16** (1965) 101.
63. *Idem, Appl. Polymer Sympos.* **3** (1966) 81.
64. R. T. HUMPIDGE and B. J. TAYLOR, *J. Sci. Instrum.* **44** (1967) 457.
65. W. T. McCARVILL and J. P. BELL, *J. Adhesion* **6** (1974) 185.
66. F. C. BOSSLER, N. C. FRANZBLAU and J. L. RUTHERFORD, *J. Phys. E.* **1** (1968) 829.
67. C. MYLONAS, Proceedings of the VIIth International Congress on Applied Mechanics, London, Vol. 4 (1948) p. 137.
68. N. J. DELLOIS and O. MONTOYA, *Appl. Polymer Sympos.* **19** (1972) 417.
69. F. SWANSON, *Polymer Eng. Sci.* **17** (1977) 122.
70. B. W. CHERRY and K. W. THOMSON, in "Adhesion-1" edited by K. W. Allen (Applied Science Publishers, London, 1977) p. 251.
71. S. E. GARF, V. I. MYSHKO and R. A. IUCHENKO, *Sintez-I-Fizikv-Khiniya Polimerov* **13** (1974) 162.
72. Y. INOUE and Y. KOBATAKE, *Appl. Sci. Res.* **A7** (1958) 53.
73. A. C. ELM, *Official Digest* **28** (1956) 752.
74. N. A. DE BRUYNE, *J. Appl. Chem.* **6** (1956) 303.
75. Y. INOUE and Y. KOBATAKE, *Appl. Sci. Res.* **A7** (1958) 314.
76. *Idem, Kolloid Z.* **18** (1958) 18.
77. H. DANNEBERG, *SPE J.* **21** (1965) 669.
78. S. GUSMAN, *Official Digest* **34** (1962) 884.
79. J. J. BIKERMAN, in "The Science of Adhesive Joints" (Academic Press, New York and London, 1968) p. 192.
80. W. C. WAKE, *Trans. I.R.I.* **35** (1959) 145.
81. J. A. CARLSON and L. P. SAPETTA, *Adhesives Age* **19**(12) (1967) 26.
82. M. H. STONE, "Adhesion and Adhesives: Science Technology and Applications" (Plastics and Rubber Institute, London, 1980) p. 101.
83. L. GREENWOOD, T. R. BOAG and A. S. McLAREN, "Adhesion, Fundamentals and Practice" (McLaren, London, 1969) p. 273.
84. J. F. KNOTT, "Fundamentals of Fracture Mechanics" (Butterworths, London, 1973) p. 94.
85. J. G. WILLIAMS, "Stress Analysis of Polymers" 2nd edn (Ellis Horwood, Chichester, 1980) p. 291.
86. A. N. GENT, *Rubb. Chem. Technol.* **47** (1974) 202.
87. A. J. KINLOCH and S. J. SHAW, in "Developments in Adhesives-2" edited by A. J. Kinloch (Applied Science Publishers, London, 1981) p. 82.
88. G. P. ANDERSON, S. J. BENNETT and K. L. DEVRIES, "Analysis and Testing of Adhesive

Bonds" (Academic Press, New York and London, 1977).
89. A. A. GRIFFITH, *Phil. Trans. Roy. Soc.* **A221** (1920) 163.
90. E. OROWAN, *Rep. Progr. Phys.* **12** (1948) 185.
91. G. R. IRWIN, *Appl. Mats. Res.* **3** (1964) 65.
92. R. S. RIVLIN and A. G. THOMAS, *J. Polymer Sci.* **10** (1953) 291.
93. A. N. GENT, A. AHAGON, N. J. KIM and Y. KUMAGI, *Rubb. Chem. Technol.* **48** (1975) 896.
94. J. R. RICE, in "Fracture – An Advanced Treatise" Vol. 2, edited by H. Liebowitz (Academic Press, New York and London, 1968) p. 191.
95. E. H. ANDREWS (ED), in "Developments in Polymer Fracture-1" (Applied Science Publishers, London, 1979) p. 1.
96. H. W. WESTERGAARD, *J. Appl. Mech. A* **6** (1939) 46.
97. D. P. ROOKE and D. J. CARTWRIGHT, "Compendium of Stress Intensity Factors" (HMSO, London, 1976) p. 7.
98. H. TADA, P. C. PARIS and G. R. IRWIN, "The Stress Analysis of Cracks Handbook" (Del Research Corporation, Hellertown, PA, 1973) p. 1.
99. F. ERDOGAN, *Eng. Fract. Mech.* **4** (1972) 811.
100. H. T. CORTEN, in "Fracture – An Advanced Treatise" Vol. 7, edited by H. Liebowitz (Academic Press, New York and London, 1972) p. 676.
101. J. G. WILLIAMS, *Adv. Polymer Sci.* **27** (1978) 68.
102. G. G. TRANTINA, *J. Compos. Mater.* **6** (1972) 192.
103. S. S. WANG, J. F. MANDELL and F. J. McGARRY, *Int. J. Fract.* **14** (1978) 39.
104. G. G. TRANTINA, *J. Composite Mater.* **6** (1972) 371.
105. K. ARIN and F. ERDOGAN, *Int. J. Eng. Sci.* **9** (1971) 213.
106. E. WU and R. L. THOMAS, Proceedings of the 5th International Congress on Rheology, Kyoto, 1968 Vol. 1 (University Park Press, Baltimore, 1969) p. 575.
107. A. PIVA and E. VIOLA, *Eng. Fract. Mechs.* **13** (1980) 143.
108. S. G. SAWYER and R. B. ANDERSON, *ibid.* **4** (1972) 605.
109. P. B. LINDLEY, *J. Inst. Rubber Ind.* **5** (1971) 243.
110. T. HATA, M. GAMO and Y. DOI, *Kobienshi Kagaku* **22** (1965) 152.
111. B. V. DERYAGUIN and N. A. KROTOVA, *Doklady Akad. Nauk SSSR* **61** (1948) 849.
112. A. N. GENT and G. R. HAMED, *J. Appl. Polymer Sci.* **21** (1977) 2817.
113. A. N. GENT and A. J. KINLOCH, *J. Polymer Sci.* **A-29** (1971) 659.
114. E. H. ANDREWS and A. J. KINLOCH, *Proc. Roy. Soc.* **A332** (1973) 385.
115. *Idem, ibid.* **A332** (1973) 401.
116. *Idem, J. Polymer Sci., Sympos.* **46** (1974) 1.
117. E. H. ANDREWS and N. E. KING, *J. Mater. Sci.* **11** (1976) 2004.
118. H. DANNEBERG, *J. Appl. Polymer Sci.* **14** (1961) 125.
119. B. M. MALYSHEV and R. L. SALGANIK, *Int. J. Fract. Mechs.* **1** (1965) 114.
120. M. L. WILLIAMS, *J. Appl. Polymer Sci.* **13** (1969) 29.
121. *Idem, ibid.* **14** (1970) 1121.
122. *Idem, J. Adhesion* **5** (1973) 81.
123. S. J. BENNETT, K. L. DEVRIES and M. L. WILLIAMS, *Int. J. Fract.* **10** (1974) 33.
124. G. P. ANDERSON, K. L. DEVRIES and M. L. WILLIAMS, *J. Coll. Interf. Sci.* **47** (1974) 600.
125. G. P. ANDERSON, S. J. BENNETT and K. L. DEVRIES, "Analysis and Testing of Adhesive Bonds" (Academic Press, New York and London, 1977) p. 58.
126. E. ANDREWS and A. STEVENSON, *J. Mater. Sci.* **13** (1978) 1680.
127. J. D. BURTON, W. B. JONES and M. L. WILLIAMS, *Trans. Soc. Rheol.* **15** (1971) 39.
128. S. J. BENNETT, G. P. ANDERSON and M. L. WILLIAMS, *J. Appl. Polymer Sci.* **14** (1970) 735.
129. M. L. WILLIAMS, K. L. DEVRIES and R. R. DESPAIN, *J. Dent. Res.* **52** (1973) 517.
130. G. P. ANDERSON, S. J. BENNETT and K. L. DEVRIES, "Analysis and Testing of Adhesive Bonds" (Academic Press, New York and London, 1977) p. 185.
131. M. L. WILLIAMS, *J. Adhesion* **3** (1972) 1.
132. T. KUNIO and M. L. WILLIAMS, Proceedings of the International Symposium on the Science and Technology of Space, Tokyo, Japan, August 1969 (1970) p. 217.
133. K. L. JOHNSON, K. KENDALL and A. D. ROBERTS, *Proc. Roy. Soc.* **A324** (1971) 301.
134. D. MAUGIS and M. BARQUINS, *J. Phys. D* **11** (1978) 1989.
135. A. D. ROBERTS and A. G. THOMAS, in "Adhesion-1" edited by K. W. Allen (Applied Science Publishers, London, 1977) p. 141.
136. K. N. G. FULLER and D. TABOR, *Proc. Roy. Soc.* **A345** (1975) 327.
137. E. J. RIPLING, S. MOSTOVOY and P. L. PATRICK, *Mat. Res. Stds* **4** (1964) 129.
138. *Idem, A.S.T.M., S.T.P.* **360** (1964) 5.
139. S. MOSTOVOY and E. J. RIPLING, *J. Appl. Polymer Sci.* **10** (1966) 1351.
140. S. MOSTOVOY, P. B. CROSLEY and E. J. RIPLING, *J. Mater.* **2** (1965) 661.
141. S. MOSTOVOY and E. J. RIPLING, Report Number N00019-75-C-0271, Naval Air Systems Command, Washington, U.S.A., 1975.
142. T. R. BRUSSAT, S. T. CHIN and S. MOSTOVOY, Report Number TR-77-162, Air Force Materials Laboratory, Dayton, U.S.A., 1977.
143. W. D. BASCOM, J. L. BITNER, R. J. MOULTON and A. R. SIEBERT, *Composites* **11** (1980) 9.
144. Y. W. MAI, *J. Adhesion* **7** (1975) 141.
146. E. H. ANDREWS and A. STEVENSON, in "Adhesion-3" edited by K. W. Allen (Applied Science Publishers, London, 1979) p. 81.
147. E. H. ANDREWS and A. STEVENSON, *J. Adhesion* **11** (1980) 17.
148. M. L. WILLIAMS, *Int. J. Fract. Mechs.* **10** (1974) 33.
149. W. D. BASCOM, R. L. COTTINGTON and C. O. TIMMONS, *Appl. Polymer Symposium* **32** (1977) 165.

150. D. R. MULVILLE, D. L. HUNSTON and P. W. MAST, *J. Eng. Mat. Technol.* **100** (1978) 25.
151. Y. W. MAI and A. S. VIPOND, *J. Mater. Sci.* **13** (1978) 2280.
152. A. D. JONATH, in "Adhesion and Adsorption of Polymers" Part A, edited by L. H. Lee (Plenum Press, New York, 1980) p. 175.
153. W. D. BASCOM, C. O. TIMMONS and R. L. JONES, *J. Mater. Sci.* **10** (1975) 1037.
154. W. D. BASCOM and J. OROSHNIK, *ibid.* **13** (1978) 1411.
155. R. A. GLEDHILL, A. J. KINLOCH, S. YAMINI and R. J. YOUNG, *Polymer* **19** (1978) 574.
156. R. A. GLEDHILL and A. J. KINLOCH, *Polymer Eng. Sci.* **19** (1979) 82.
157. W. D. BASCOM, R. L. COTTINGTON, R. L. JONES and P. PEYSER, *J. Appl. Polymer Sci.* **19** (1975) 2545.
158. W. D. BASCOM and R. L. COTTINGTON, *J. Adhesion* 7 (1976) 333.
159. W. D. BASCOM, R. L. COTTINGTON and C. O. TIMMONS, *Naval. Eng. J.* 88 (1976) 73.
160. D. L. HUNSTON, J. L. RUSHFORD, J. L. BITNER and J. OROSHNIK, *J. Elastomers Plast.* **12** (1980) 133.
161. A. J. KINLOCH and S. J. SHAW, *J. Adhesion* **12** (1981) 59.
162. D. L. HUNSTON, J. L. BITNER, W. S. ROSE, J. L. RUSHFORD and C. K. RIEW, *ibid.* **13** (1981) to be published.
163. J. N. SULTAN and F. J. McGARRY, *Polymer Eng. Sci.* **13** (1973) 29.
164. R. DRAKE and A. SIEBERT, *SAMPE Quart.* **6**(4) (1975) 11.
165. S. MOSTOVOY and E. J. RIPLING, *Appl. Polymer Symp.* **19** (1972) 395.
166. M. TAKASHI, K. OGAWA, R. KATITA and T. KUNO, Proceedings of the Japan Congress on Materials Research **16** (1973) 211.
167. R. A. GLEDHILL, A. J. KINLOCH and S. J. SHAW, *J. Mater. Sci.* **14** (1979) 1769.
168. S. MOSTOVOY and E. J. RIPLING, *J. Appl. Polymer Sci.* **13** (1979) 1083.
169. E. J. RIPLING, S. MOSTOVOY and C. BERSCH, *J. Adhesion* **3** (1971) 145.
170. A. J. KINLOCH, R. A. GLEDHILL and W. A. DUKES, in "Adhesion, Science and Technology" edited by L. H. Lee (Plenum Press, New York, 1975) p. 597.
171. B. W. CHERRY and K. W. THOMSON, "Fracture Mechanics and Technology (Sijthoff and Nordoff, Netherlands, 1971) p. 723.
172. A. J. KINLOCH, *J. Adhesion* **10** (1979) 193.
173. R. A. GLEDHILL, A. J. KINLOCH and S. J. SHAW, *ibid.* **11** (1980) 3.
174. J. C. McMILLAN, in "Developments in Adhesives-2" edited by A. J. Kinloch (Applied Science Publishers, London, 1981) p. 243.
175. R. O. EMBEWLE, B. H. RIVER and J. A. KOUTSKY, *Wood Fiber* **11** (1979) 197.
176. *Idem, ibid.* **12** (1980) 40.
177. D. R. MULVILLE and R. VAISHNAV, *J. Adhesion* **7** (1975) 215.
178. M. TAKASHI, K. OGAWA and T. KUMO, Proceedings of the Japan Congress on Materials Research, Vol. 17, 1974, p. 192.
179. R. L. PATRICK, J. A. BROWN, N. M. CAMERON and W. G. GEHMAN, *Appl. Polymer Sympos.* **16** (1971) 87.
180. R. L. PATRICK (ED), "Treatise on Adhesion and Adhesives" Vol. 4 (Marcel Dekker, New York, 1973) 163.
181. R. C. WILCOX and W. A. JEMAIN, *Polymer Eng. Sci.* **13** (1973) 40.
182. R. W. BRYANT and W. A. DUKES, Aeronautic and Space Engineering and Manufacturing Meeting, Los Angeles, October 1967, Paper No. 670855 (SAE, New York, 1968).
183. H. P. MEISSNER and G. H. BALDAUF, *Trans. ASME* **73** (1951) 697.
184. N. BREDZS and H. SCHWARTZBART, *Welding J. (Welding Res. Suppl.)* (1956) 610.
185. H. P. MEISSNER and E. W. MERRILL, *ASTM Bull.* **151** (1948) 80.
186. S. W. LOSOSKI and G. KRUAS, *J. Polymer Sci.* **18** (1955) 359.
187. A. G. H. DIETZ, *ASTM, STP* **194** (1957) 19.
188. J. J. BIKERMAN and C. R. HUANG, *Trans. Soc. Rheol.* **3** (1959) 5.
189. J. J. BIKERMAN, "The Science of Adhesive Joints" (Academic Press, New York and London, 1968) p. 273.
190. W. A. DUKES and R. W. BRYANT, *J. Adhesion* **1** (1969) 48.
191. W. C. WAKE, in "Adhesion" edited by D. D. Eley (Oxford University Press, London, 1961) p. 191.
192. A. N. GENT, *J. Polymer Sci.* **A2** (1974) 283.
193. P. D. HILTON and G. D. GUPTA, "Design and Engineering Conference" Philadelphia, April 1973, Paper No. 73-De-21 (ASME, Philadelphia, 1973).
194. R. D. ADAMS and J. COPPENDALE, *J. Adhesion* **10** (1979) 49.
195. N. A. DEBRUYNE, *Aircraft Eng.* **16** (1944) 115.
196. *Idem, ibid.* **16** (1944) 140.
197. K. WELLINGER and U. REMBOLD, *VDI Zeitschrift* **100** (1958) 41.
198. A. N. GENT and G. R. HAMED, *Polymer Eng. Sci.* **17** (1977) 462.
199. J. JOHNSTON, *Adhesives Age* **11**(4) (1968) 20.
200. D. W. AUBREY, G. N. WELDING and T. WONG, *J. Appl. Polymer Sci.* **13** (1969) 2193.
201. T. IGARASHI, *ibid.* **19** (1975) 2129.
202. F. YAMAMOTO, S. YAMAKAWA and S. TSURU, *J. Polymer Sci. Polymer Phys. Ed.* **18** (1980) 1847.
203. D. SATAS and F. EGAN, *Adhesives Age* **9**(8) (1966) 22.
204. G. J. LAKE and A. STEVENSON, *J. Adhesion* **12** (1981) 13.
205. D. W. AUBREY, T. A. JACKSON and J. D. SMITH, *J. Inst. Rubber. Ind.* **3** (1969) 265.
206. K. KENDALL, *J. Phys. D. Appl. Phys.* **11** (1978) 1519.
207. R. W. ATKINS, A. J. KINLOCH and S. J. SHAW, unpublished work, 1980.
208. D. H. KAELBLE, *J. Colloid Sci.* **19** (1969) 102.
209. D. H. KAELBLE and R. S. REYLEK, *J. Adhesion* **1**

(1969) 124.
210. A. N. GENT and R. P. PETRICH, *Proc. Roy. Soc.* **A310** (1969) 433.
211. D. W. AUBREY and M. SHERRIFF, *J. Polymer Sci. Polymer Chem. Ed.* **18** (1980) 2597.
212. R. BATES, *J. Appl. Polymer Sci.* **20** (1976) 2941.
213. M. L. WILLIAMS, R. F. LANDEL and J. D. FERRY, *J. Amer. Chem. Soc.* **77** (1955) 3701.
214. D. W. AUBREY, in "Adhesion-3" edited by K. W. Allen (Applied Science Publishers, London, 1979) p. 191.
215. J. L. COTTER, *Revs. High Temp. Mat.* **3**(4) (1973) 277.
216. J. C. BOLGER, in "Treatise on Adhesion and Adhesives" Vol. 3, edited by R. L. Patrick (Marcel Dekker, New York, 1973) p. 1.
217. R. E. YAEGER, *Appl. Polymer Sympos.* **3** (1969) 369.
218. S. R. SANDLER and F. R. BERG, *J. Appl. Polymer Sci.* **9** (1965) 3909.
219. A. F. LEWIS, R. A. KINMONTH and R. P. KREAHLING, *J. Adhesion* **3** (1972) 249.
220. A. F. LEWIS, *Adhesives Age* **15**(6) (1972) 38.
221. K. W. ALLEN and M. E. R. SHANAHAN, *J. Adhesion* **7** (1975) 161.
222. *Idem, ibid.* **8** (1976) 43.
223. W. SPATH, *Adhäsion* **17**(10) (1973) 348.
224. V. RAYATSKAS and V. PEKARSKAS, *J. Appl. Polymer Sci.* **20** (1976) 1941.
225. J. P. THOMAS, *Appl. Polymer Sympos.* **3** (1969) 109.
226. W. C. WAKE, K. W. ALLEN and S. M. DEAN, in "Elastomers: Criteria for Engineering Design" edited by C. Hepburn and R. J. W. Reynolds (Applied Science Publishers, London, 1979) p. 311.
227. R. A. GLEDHILL and A. J. KINLOCH, *Polymer* **17** (1976) 727.
228. J. R. ROMANKO and W. G. KNAUSS, in "Developments in Adhesives-2" edited by A. J. Kinloch (Applied Science Publishers, London, 1981) p. 173.
229. J. R. BEATTY and E. C. DALGUISH, *Rubb. Chem. Technol.* **47** (1974) 188.
230. R. J. KUHBANDER and T. J. APONYI, *Adhesives Age* **19**(9) (1976) 27.
231. J. A. MARCEAU, *ibid.* **21**(4) (1978) 37.
232. J. PETERKA, *Adhäsion* **17** (1973) 288.
233. W. SPATH, *ibid.* **16** (1972) 416.
234. W. D. BASCOM and S. MOSTOVOY, *Amer. Chem. Soc., Organic Coatings Plastics Chem., Prepr.* **38** (1978) 152.
235. A. J. KINLOCH and J. G. WILLIAMS, *J. Mater. Sci.* **15** (1980) 987.
236. A. J. KINLOCH, *Metal Sci.* **14** (1980) 305.
237. S. MOSTOVOY and E. J. RIPLING, in "Adhesion, Science and Technology" Part B, edited by L. H. Lee (Plenum Press, New York, 1975) p. 513.
238. N. J. DELOLLIS, *Adhesives Age* **20**(9) (1977) 41.
239. J. D. MINFORD, *ibid.* **21**(3) (1978) 17.
240. W. D. BASCOM, *ibid.* **22**(4) (1979) 28.
241. R. J. SCHLIEKELMANN (ED), "Bonded Joints and Preparation for Bonding" (NATO-AGARD, Lecture Series 102, 1979).
242. R. A. GLEDHILL and A. J. KINLOCH, *J. Adhesion* **6** (1974) 315.
243. D. H. KAELBLE, *J. Appl. Polymer Sci.* **18** (1974) 1869.
244. D. K. OWENS, *ibid.* **14** (1970) 1725.
245. M. GETTINGS, F. S. BAKER and A. J. KINLOCH, *ibid.* **21** (1977) 2375.
246. A. N. GENT and J. SCHULTZ, *J. Adhesion* **3** (1972) 281.
247. S. N. ZHURKOV and E. E. TOMASHEVSKY, "Physical Basis of Yield and Fracture" (Institute of Physics, London, 1966) p. 200.
248. S. N. ZHURKOV and U. E. KORSUKOV, *J. Polymer Sci. Polymer Phys.* **12** (1974) 385.
249. D. W. LEVI, R. F. WEGMAN, M. C. ROSS and E. A. GARNIS, *SAMPE Quart.* **7**(3) (1971) 1.
250. W. D. BASCOM, S. T. GADOMSKI, C. M. HENDERSON and R. L. JONES, *J. Adhesion* **8** (1977) 213.
251. F. J. RIEL, *SAMPE J.* **7** (1971) 16.
252. J. L. COTTER, in "Developments in Adhesives-1" edited by W. C. Wake (Applied Science Publishers, London, 1977) p. 1.
253. R. W. SHANNON and E. W. THRALL, *J. Appl. Polymer Sci., Appl. Polymer Sympos.* **32** (1977) 131.
254. J. S. NOLAND, "Adhesion, Science and Technology" edited by L. H. Lee (Plenum Press, New York, 1975) p. 413.
255. J. D. VENABLES, D. K. McNAMARA, T. S. SUN, B. DATCHEK and J. M. CHEN, "Structural Adhesives and Bonding Technology" (Technical Conference Associates, El Segundo, California, 1979) p. 12.
256. T. S. SUN, J. M. CHEN, J. D. VENABLES and R. HOPPING, *Appl. Surf. Sci.* **1** (1978) 202.
257. A. J. KINLOCH and N. J. SMART, *J. Adhesion* **12** (1981) 23.
258. J. D. MINFORD, *Adhesives Age* **17**(7) (1974) 24.
259. J. A. SMITH and W. E. MARTINSEN, *Amer. Ceram. Soc. Bull.* **52** (1973) 855.
260. J. C. COMYN, in "Developments in Adhesives-2" edited by A. J. Kinloch (Applied Science Publishers, London, 1981) p. 279.
261. D. M. BREWIS, J. COMYN, B. C. COPE and A. C. MOLONEY, *Polymer* **21** (1980) 344.
262. J. COMYN, D. M. BREWIS, R. J. A. SHALASH and J. L. TEGG, in "Adhesion-3" edited by K. W. Allen (Applied Science Publishers, London, 1979) p. 13.
263. D. M. BREWIS, J. COMYN and J. L. TEGG, *Int. J. Adhes. Adhesives* **1** (1980) 35.
264. D. M. BREWIS, J. COMYN, B. C. COPE and A. C. MOLONEY, *Polymer* **21** (1980) 1477.
265. W. ALTHOF, *Nat. SAMPE Tec. Conf.* **11** (1979) 309.
266. *Idem, Aluminium* **55** (1979) 600.
267. D. M. BREWIS, J. COMYN, A. C. MOLONEY and J. L. TEGG, *Eur. Polymer J.* **17** (1981) 127.
268. B. W. CHERRY and K. W. THOMSON, "Fracture Mechanics and Technology" (Sijthoff and Nordoff, Netherlands, 1977) p. 723.
269. J. A. BARRIE, in "Diffusion in Polymers" edited by J. Crank and G. S. Park (Academic Press, New York and London, 1968) p. 259.

270. M. GETTING and A. J. KINLOCH, *J. Mater. Sci.* **12** (1977) 2049.
271. *Idem, Surf. Interface Anal.* **1** (1980) 189.
272. J. C. BOLGER and A. S. MICHAELS, in "Interface Conversion for Polymer Coatings" edited by P. Weiss and G. D. Cheever (Elsevier, Amsterdam, New York and Oxford, 1968) p. 3.
273. B. F. LEWIS, W. M. BROWSER, J. L. HORN, T. LUU and W. H. WEINBERG, *J. Vac. Sci. Technol.* **11**(1974) 262.
274. J. C. McMILLAN and J. T. QUINLIVAN, *SAMPE Quart.* 7(3) (1976) 13.
275. A. W. BETHUNE, *SAMPE J.* **11**(4) 1975) 4.
276. J. D. VENABLES, D. K. McNAMARA, J. M. CHEN, T. S. SUN and R. L. HOPPING, *Appl. Surf. Sci.* **3** (1979) 88.
277. W. BRQCKMAN and H. KOLLEK, Proceedings of the 23rd National SAMPE Symposium, 1978 (SAMPE, San Francisco, 1978) p. 1119.

Received 20 May
and accepted 21 July 1981